CyAは1日2分割で投与されていた。PSLは，全例最初から2倍量投与に変更されていた。CyAについてはRFP開始前のCyAトラフ値を目標として，トラフ値を測定しながら投与量の変更が行われていた。

以下，症例ごとに経過を示す。

症例1（Fig. 1）：69歳女性。平成8年より強皮症・間質性肺炎に対してPSL開始され，平成14年よりCyA併用となり，PSL 7.5 mg/日，CyA 100 mg/日使用しCyAトラフ値100 ng/ml前後でコントロール良好であった。平成15年6月肺結核（bⅡ1）発症し，抗結核薬としてHREを開始。PSLを15 mg/日に増量，CyAを200 mg/日に増量したが，CyAトラフ値は50 ng/ml前後と低値を示した。CyAトラフ値測定を繰り返し，最終的に7週後にCyA 300 mg/日使用しCyAトラフ値100 ng/ml前後でコントロール良好となった。その時点までにトラフ値測定は8回行われていた。

症例2（Fig. 2）：78歳男性。平成16年3月間質性肺炎急性増悪に対して治療開始され，PSL 20 mg/日，CyA 150 mg/日使用しCyAトラフ値100 ng/ml前後でコントロール良好であった。同年6月肺結核（bⅢ2）発症し，抗結核薬としてHREを開始。PSLを40 mg/日に増量，CyAを250 mg/日に増量したが，CyAトラフ値40 ng/ml前後と低値のため，CyAをさらに増量した。経過中，薬疹出現にてHREを一時休薬し，INH＋EBとレボフロキサシン（LVFX）に変更し，RFPは減感作成功後に常用量に戻した。最終的に12週後にCyA 450 mg/日使用しCyAトラフ値100 ng/ml前後となりコントロール良好となった。その時点までにトラフ値測定は8回行われて

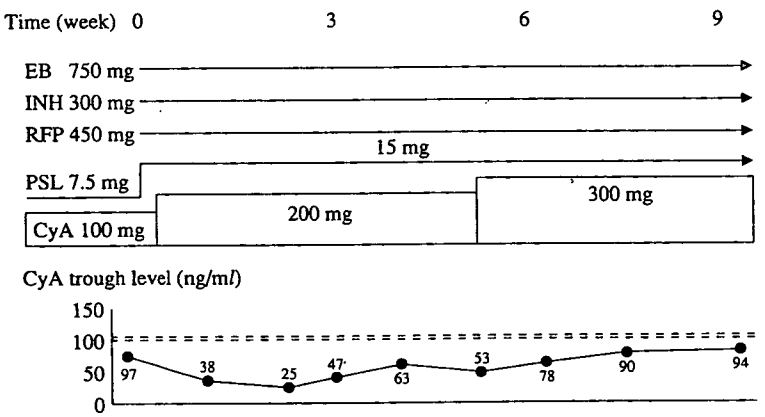


**Fig. 1** Daily dose of CyA during anti-tuberculosis treatment containing RFP to maintain optimum CyA trough level (case 1: a 69-year-old woman with scleroderma and interstitial pneumonia)
EB: ethambutol, INH: isoniazid, RFP: rifampicin, PSL: prednisolone, CyA: cyclosporine

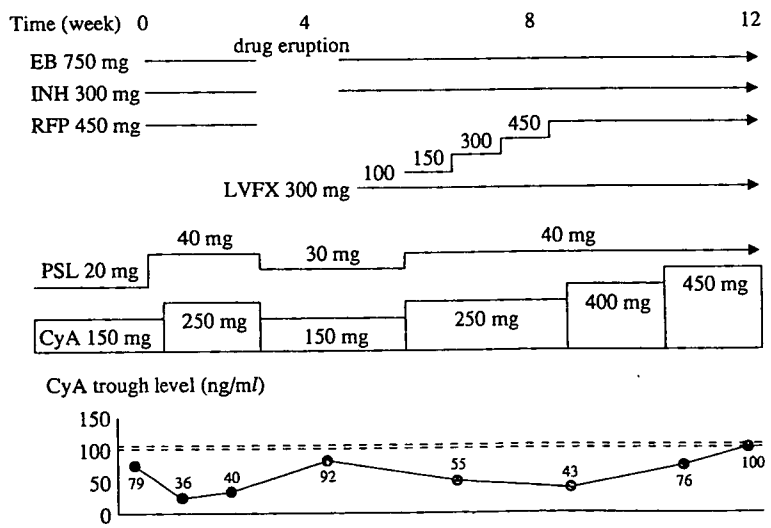


**Fig. 2** Daily dose of CyA during anti-tuberculosis treatment containing RFP to maintain optimum CyA trough level (case 2: a 78-year-old man with idiopathic pulmonary fibrosis)
LVFX: levofloxacin

いた。

症例3（Fig. 3）：51歳男性。平成15年5月間質性肺炎急性増悪に対して治療開始され，PSL 15 mg/日，CyA 200 mg/日使用し，CyAトラフ値100 ng/ml前後でコントロール良好であった。同年7月肺結核（*b*III2）発症し，抗結核薬としてHREを開始。本例はPSL減量中であったため，一時的にPSLを30 mg/日に増量してから，再び減量を行った。CyAトラフ値は安定せず，CyAの増量を繰り返した。最終的に27週後CyA700 mg/日使用しCyAトラフ値100 ng/ml前後でコントロール良好となった。その時点までにトラフ値測定は12回行われていた。

症例4（Fig. 4）：71歳女性。平成15年よりSLEにてPSL開始され，平成16年よりCyA併用となり，PSL 30 mg/日，CyA 100 mg/日にてCyAトラフ値40 ng/ml前後でコントロール良好であった。同年7月肺結核（*b*III3）発症し，抗結核薬としてHREZを開始。本例もPSL減量中にて一時的にPSL 60 mg/日に増量してから減量を行った。CyAは150 mg/日に増量したがCyAトラフ値30 ng/ml前後と低値のため，さらに増量した。最終的に6週後にCyA 250 mg/日使用しCyAトラフ値40 ng/ml前後でコントロール良好となった。その時点までにトラフ値測定は5回行われていた。

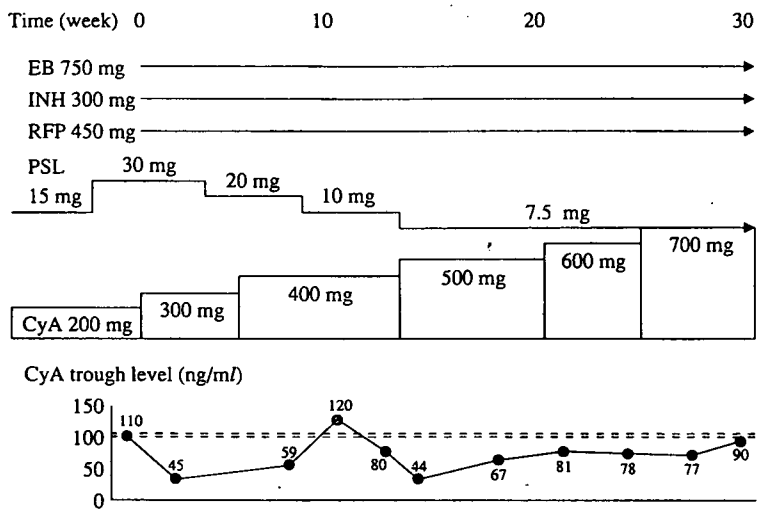


**Fig. 3** Daily dose of CyA during anti-tuberculosis treatment containing RFP to maintain optimum CyA trough level (case 3: a 51-year-old man with idiopathic pulmonary fibrosis)

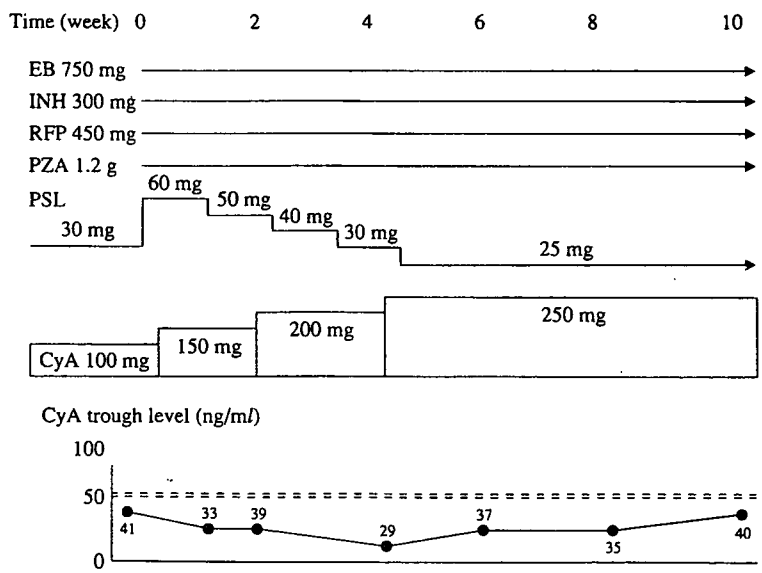


**Fig. 4** Daily dose of CyA during anti-tuberculosis treatment containing RFP to maintain optimum CyA trough level (case 4: a 71-year-old woman with systemic lupus erythematodes)

Table Clinical data of 4 patients about cyclosporine

| Case | Sex | Age (yr) | RFP dose (mg/day) | RFP (−) CyA dose (mg/day) | RFP (+) final CyA dose (mg/day) | To reach final CyA trough levels | |
|---|---|---|---|---|---|---|---|
| | | | | | | Frequency of measurement (times) | Periods (week) |
| 1 | F | 69 | 450 | 100 | 300 | 8 | 7 |
| 2 | M | 78 | 450 | 150 | 450 | 8 | 12 |
| 3 | M | 51 | 450 | 200 | 700 | 12 | 27 |
| 4 | F | 71 | 450 | 100 | 250 | 5 | 6 |
| | | | | | Average | 8.3 | 13 |

CyA: cyclosporine, RFP: rifampicin

4症例とも肺結核の経過は順調で，全例化療開始1カ月後に菌陰性化した。また，いずれの症例においても原疾患の悪化，副作用は認めなかった。

以上をまとめると（Table），結核化療開始時にPSLは全例で2倍に増量されていた。一方CyAは化療開始時に1.5～2倍に増量された後，投与量の変更を頻回に繰り返されていた。最終的にCyAは2.5～3.5（平均3）倍量でトラフ値が目標値（化療開始前の値）に達し，投与量が定まった。CyAトラフ値測定は5～12（平均8.3）回施行され，安定までに6～27（平均13）週を要していた。

## 考　　案

近年ステロイド，免疫抑制剤使用の増加に伴いimmunocompromised hostも多くなっている。今回の4例も基礎疾患に間質性肺炎や膠原病があり，ステロイドと免疫抑制剤CyA投与中に日和見感染として肺結核が発症し，RFPを含む抗結核療法が開始されている。このような場合問題となるのが，ステロイドおよびCyAとRFPとの薬物相互作用である。RFPは，肝臓におけるチトクロームP450系の様々なアイソザイムをふくむ多様な代謝経路を誘導する物質として知られている[1)~3)]。RFP投与により代謝酵素の活性が誘導され，薬剤によっては代謝を受けることにより血中濃度が低下し，その薬剤として期待されていた治療域に達しないことが生じる[4)]。また，投与開始から肝酵素が誘導されるまでに数日から2週間ほどかかり，投与を中止しても影響が消失するまでにも同様の日数を要するとされている。

ステロイド類はRFPの併用により半減期が短縮するといわれている。ステロイドの種類により短縮率は異なるが，PSLにおいては短縮率44%で，必要量は2倍になるという報告がある[5)6)]。今回のわれわれの結果においても，PSLはこれまでの推奨どおり全例2倍量に増量されていた。

一方CyAに関しては，1990年にAl-Sulaimanらにより腎移植患者6例において約3～5倍に増量したという報告と[7)]，1998年にKimらにより腎移植患者4例において約2.5～3倍に増量したという報告がなされている[8)]。いずれも海外の腎移植患者におけるRFP 600 mg/日併用時の報告であり，多くがRFP 450 mg/日を使用している本邦での報告は未だない。

免疫抑制剤CyAは，主としてT細胞（ヘルパーT細胞）によるインターロイキン-2（IL-2）などのサイトカイン産生を阻害することにより強力な免疫抑制作用を示すとされているが，免疫抑制効果を期待できる血中濃度と中毒域との差が小さい。そのためCyAを効果的に用いるには，トラフ値で代表されるように全血で血中濃度をモニタリングして投与量を決定しなければならない[9)]。RFPとの併用開始後，RFPの影響が最大となるまでに数日から2週間程度を要し，RFP中止4～7日後までCyA濃度の低下が認められ，CyAの濃度回復に平均10日を要すると報告されている[10)]。また，RFPとの併用開始後CyAの血中濃度が低下し原疾患の悪化を認めたとの報告もある[11)]。したがって，RFPとの併用時には慎重にCyAの投与量を決める必要がある。

今回のわれわれの検討では，RFP 450 mg/日併用時にはCyAは最終的に投与量を2.5～3.5倍（平均3倍）に増量することにより，CyAトラフ値がRFP投与前の値に到達し，臨床的にも安定した状態を保つことができた。また，RFP開始しCyA増量後6～12日（平均7日）後には，CyAトラフ値がRFP投与前の値に到達した。しかしながら，CyA投与量決定までに6～27週（平均13週），CyAトラフ値測定も5～12回（平均8.3回）を要しており，きわめて非効率的であった。これらの結果より本邦においては，RFP併用開始時にはCyAを数日～2週間以内に3倍量に増量し，約7日後のCyAトラフ値を参考にして微調整すれば効率よく適切なCyA投与量を決めることが可能と思われた。

## 文　　献

1) Bachmann KA, Jauregui L: Use of single sample clearance estimates of cytochrome P450 substrates to characterize human hepatic CYP status *in vivo*. Xenobiotica. 1993 ; 23 : 307–315.

2) Caraco Y, Sheller J, Wood AJ: Pharmacogenetic Determination of Codeine Induction by Rifampin: The Impact on Codeine's Respiratory, Psychomotor and Miotic Effects. 1997 ; 281 : 330–336.
3) Dilger K, Greiner B, Fromm MF, et al.: Consequences of rifampicin treatment on propafenone disposition in extensive and poor metabolizers of CYP2D6. Pharmacogenetics. 1999 ; 9 : 551–559.
4) Strayhorn VA, Baciewicz AM, Self TH: Update on Rifampin Drug Interactions, Ⅲ. Arch Intern Med. 1997 ; 157 : 2453–2458.
5) 河合眞一, 市川陽一, 本間光夫：リファンピシン併用によりステロイド治療抵抗性を示した膠原病症例とその薬物速度論的分析. リウマチ. 1984 ; 24 : 32–37.
6) 河合眞一：リファンピシン服用者における各種糖質コルチコイド代謝動態の比較. 日内分泌会誌. 1985 ; 61 : 145–161.
7) Al-Sulaiman MH, Dhar JM, Al-Khader AA: Successful use of rifampicin in the treatment of tuberculosis in renal transplant patients immunosuppressed with cyclosporine. Transplantation. 1990 ; 50 : 597–598.
8) Kim YH, Yoon YR, Kim YW, et al.: Effects of rifampin on cyclosporine disposition in kidney recipients with tuberculosis. Transplantation Proceedings. 1998 ; 30 : 3570–3572.
9) Hebert MF, Roberts JP: Bioavailability of cyclosporine with concomitant rifampin administration is markedly less than predicted by hepatic enzyme induction. J Clin Pharmacol. 1992 ; 52 : 453–457.
10) Zelunka EJ: Intravenous Cyclosporine-Rifampin Interaction in a Pediatric Bone Marrow Transplant Recipient. Pharmacotherapy. 2002 ; 22 : 387–390.
11) Offermann G, Keller F, Molzahn M: Low cyclosporine blood levels and acute graft rejection in a renal transplant patient recipient during rifampin treatment. Am J Nephrol.

**Original Article**

# EXAMINATION OF ADMINISTRATIVE DOSAGE OF CYCLOSPORINE DURING THE ANTI-TUBERCULOSIS CHEMOTHERAPY INCLUDING RIFAMPICIN

[1,2]Yoshinori MATSUI, [1]Shinobu AKAGAWA, [1]Masahiro KAWASHIMA, [1]Junko SUZUKI, [1]Kimihiko MASUDA, [1]Atsuhisa TAMURA, [1]Hideaki NAGAI, [1]Naohiro NAGAYAMA [1]Yoshiko KAWABE, [1]Kazuko MACHIDA, [1]Atsuyuki KURASHIMA, and [1]Hideki YOTSUMOTO

**Abstract** [Aims] In the treatment of tuberculosis with rifampicin in patients treated with prednisolone and cyclosporine, we have to increase the dosage of these drugs. Although prednisolone dosage is recommended to be doubled, there is no established consensus about cyclosporine dosage. Our aim is to review the current situation at our institution regarding the dosage of cyclosporine administered to tuberculous patients after the addition of rifampicin to the treatment regimen.

[Methods and Results] We reviewed patients' clinical status and how dosages of cyclosporine were altered during a course of tuberculosis treatment including rifampicin in 4 patients (2 interstitial pneumonitis, 2 collagen vascular disease) who were being treated with cyclosporine between 2001 and 2003. Prednisolone had been also administrated in all patients and the dosage was doubled from the beginning of the treatment. The appropriate dosage of cyclosporine was found to be 2.5–3.5 (average 3) times that of initial dosage, and it required 5–12 weeks (average 8.3) measurements of trough levels and 6–27 (average 12) weeks until appropriate trough levels were obtained.

[Conclusions] The appropriate dosage of cyclosporine was found to be approximately 3 times that of the initial dosage in all patients, but it required a long term and frequent measurements of trough levels before reaching this goal. It seems that trebling the dosage of cyclosporine from the start of anti-tuberculosis chemotherapy will be an efficient way to achieve good clinical outcome.

**Key words**: Rifampicin, Cyclosporine, Prednisolone, Drug interactions, Tuberculosis

[1]Department of Pulmonary Medicine, National Hospital Organization Tokyo National Hospital, [2]Department of Pulmonary Medicine, Jikei University School of Medicine

Correspondence to: Yoshinori Matsui, Department of Pulmonary Medicine, National Hospital Organization Tokyo National Hospital, 3–1–1, Takeoka, Kiyose-shi, Tokyo 204–8585 Japan. (E-mail: yoshi-matsui@nifty.com)

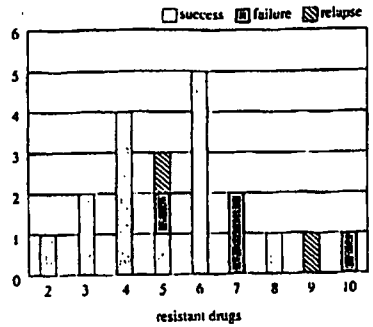


Fig. Resistant drugs and results of incomplete resections

Table 2 Background of incomplete resections

| | | Preoperative bacilli within 3 months | Resistant drugs | Residual lesion | Postoperative chemotherapy months |
|---|---|---|---|---|---|
| Success | 1 | none | 3 | nodular/infiltration | 24 |
| | 2 | none | 4 | nodular/infiltration | 19 |
| | 3 | none | 6 | nodular/infiltration | 13 |
| | 4 | culture positive | 4 | nodular/infiltration | 52 |
| | 5 | culture positive | 8 | nodular/infiltration | 22 |
| | 6 | I | 4 | nodular/infiltration | 6 |
| | 7 | II | 6 | cavity | 30 |
| | 8 | III | 5 | nodular/infiltration | 12 |
| | 9 | V | 6 | nodular/infiltration | unknown |
| | 10 | V | 6 | nodular/infiltration | 19 |
| | 11 | VI | 4 | nodular/infiltration | 6 |
| | 12 | VI | 6 | nodular/infiltration | 8 |
| | 13 | VII | 3 | nodular/infiltration | 24 |
| | 14 | VII | 2 | nodular/infiltration | 21 |
| Failure | 15 | none | 10 | nodular/infiltration | 9 |
| | 16 | culture positive | 5 | nodular/infiltration | 24 |
| | 17 | VII | 7 | nodular/infiltration | 25 |
| | 18 | IX | 7 | nodular/infiltration | 42 |
| Relapse | 19 | none | 5 | nodular/infiltration | 29 |
| | 20 | VI | 9 | nodular/infiltration | 29 |

1例，1個性病変1例（肺切除術予定であったが，理由は明らかでないが胸郭成形術なった症例）であった。術前3カ月の排菌状態は，全例が排菌陽性で，培養のみ陽性例が3例，塗抹培養とも陽性例が2例であった。術後の抗結核薬の投与期間は術後早期に死亡した1例を除くと24～120カ月であった。

（3）術後合併症

術後合併症は，肺切除31例中7例に，胸郭成形術5例中1例に発生した。そのうち，死亡に至った症例は3例であった。肺切除術後の死亡例は2例で，1例は術後膿胸を発生し非手術側肺に感染が波及したことによる結核死で，もう1例は術後の脳梗塞による死亡であった。胸郭成形術後の死亡例は，両側巨大空洞例の術後に肺結核が増悪した症例であった。死亡に至らなかった術後合併症はいずれも肺切除例に発生したものであり2例が術後出血，2例が膿胸，1例が術後は肺瘻，1例は術後神経症状の出現であった。

## 考　察

肺結核の手術件数は，抗結核剤の開発に伴い著しく減少した。しかし，多剤耐性肺結核の場合，内科的治療で治癒しうる症例もあるものの，内科的治療のみでは治癒しきれない症例も存在する。多剤耐性肺結核で治療に失敗すると単に生命予後が不良であるばかりでなく，患者も長期入院を余儀なくされ著しくQOLも低下する。そして，患者個人のみでなく社会的にも経済的にもその損失は大きなものである。多剤耐性肺結核の治療を考える場合，内科的治療のみでなく常に外科的治療の可能性も考慮に入れておくことは重要であると思われる。今回，病巣を残さず切除し得たと思われる症例では，薬剤耐性数や術前の排菌状態に関係なく排菌を陰性化させることができた。このことより，手術可能な肺機能で病巣が限局化しており手術により完全に切除可能な多剤耐性肺結核は肺切除術が妥当であり，従来の報告のとおりであった[1)2)]。また，術後の抗結核薬の投与も1年以上継続させればよいものと思われる。

肺切除症例のうち，病変を残した症例で術後再排菌を認めなかった症例は70%であった。残した病巣の性状は1例の空洞性病変を除き19例が粒状・浸潤影であった。また，治療失敗例，再発例の全例が遺残病変は粒状・浸潤影であった。中島は手術対象となる病変は吸化性空洞または径2cm以上の結核結節であるとしている[3)]。井内らは再排菌，持続排菌の症例はそのほとんどが，遺残空洞性病変を有する症例であったと述べている[4)]。しかし，今回の検討では，粒状・浸潤影でも病変を遺残させるとその30%で治療失敗や再発を認めている。病変を残した症例の薬剤耐性数は4種類以下では再排菌を認めていないが，5種類以上では治療失敗や再発を認められるようになり，7剤以上に耐性となると再排菌を認めない症例は20%に減少した。このことから，病変を残存させる可能性のある症例では耐性薬剤数が増加する前に手術に踏み切ることが必要と思われる。手術時期は，全身状態や薬剤治療の状況にもよると思われるが，十分な内科的治療を行ったうえで，4～6カ月たっても排菌が持続する場合が一般的と思われる[3)4)]。今回の検討より，病変が完全に切除可能な場合は，手術により再排菌をしなくなる可能性が高いため，排菌が陰性化しても，肺機能などより十分手術に耐えうる症例は，相対的に肺切除術の適応となりうるものと思われる[3)]。術後の抗結核薬の投与期間は，1年半から2年は必要と思われる[3)]。しかし，今回の検討では術後2年以上抗結核薬投与を行っても再発した症例もあることより術後慎重な経過観察が必要と思われる。

胸郭成形術は葉切除術ができない症例に検討されるが，十分に症例を選択すればある程度はその治療的意義はあるものと思われる。しかし，肺切除術に比較すると治療効果は低いため術後長期間の抗結核薬の投与を必要とするものと考えられる。

## ま と め

多剤耐性肺結核の手術では，病巣を完全に切除可能であれば排菌を停止させることができる可能性が高い。一方，病変を残さざるを得ない症例では，有効薬剤数が多いほど排菌を停止させうる可能性が高いので，内科的治療に抵抗性の場合は早期より外科的治療を検討することが重要である。

## 文　献

1）矢野　貢，筑井俊昭，稲垣敬三，他：肺結核外科療法不成功例の検討．結核．1997；71：35-38.
2）小松彦太郎：結核症外科治療の適応とその有効性．肺結核「結核 Up to Date」．毛利昌史，四元秀毅，倉島篤行，南江堂，東京，1999，101-104.
3）中島由槻：多剤耐性結核の治療．結核．2002；77：805-813.
4）井内敬二，前田　元，中川勝裕，他：多剤耐性肺結核の外科療法適応．THE LUNG perspectives. 1999；7：402-405.
5）McLaughlin JS, Hankins JR: Current aspects of surgery for pulmonary tuberculosis. Ann Thorac Surg. 1974；17：513-525.





## 6. 多剤耐性結核患者に対する活性化T細胞輸注療法の試み

国立国際医療センター研究所呼吸器疾患研究部　*中田　光*，濱野　栄美
*新潟大学医歯学総合病院生命科学医療センター
独立行政法人国立病院機構東京病院　川辺　芳子，益田　公彦，水井　英明，有賀　暁之，倉島　篤行
東京医科歯科大学細胞治療センター　森尾　友宏，清水　則夫

## はじめに

多剤耐性結核は，いったん感染すると治療がきわめて難しく，周囲への感染拡大の危険性もある。また，患者は長期の入院を余儀なくされており，確実な治療法として外科的肺切除を受けることが多い。さらに病変の広がり，肺機能などから外科的治療を受けられない患者では治療自体が非常に困難になる。

活性化自己T細胞輸注法は国立がんセンター研究所の岡根らにより開発された方法で，自己血中のT細胞を固相化抗CD3抗体とインターロイキン2（IL-2）の存在下で培養し，1000倍程度に増殖させた後，体内に戻すものである。現在までに，700症例以上の患者に対し，延べ7000回以上の投与が行われた。ホジキン病，肝細胞癌，卵巣腫瘍など様々な腫瘍で縮小効果を認めるとともに，慢性活動性エプスタンバールウイルス（EBV）感染症，免疫不全症に合併した化学療法抵抗性のサイトメガロウイルス（CMV）感染症，カリニ肺炎などに効果を認めている。副作用は感染症に対する反応としての発熱程度であることが多く，強い炎症が起きた場合もステロイド剤などでコントロールすることが可能であり，その安全性が東京医科歯科大学においても再確認された。このようにT細胞機能不全がある症例でもT細胞を生体外で活性化，増殖させ，生体内に戻すことによりT細胞機能を高めることが可能であることが明らかになってきている。

結核感染症に対する生体側の防御機構はT細胞を中心とする細胞性免疫が担っている。多剤耐性結核患者では細胞性免疫機能の低下が指摘されており，治療法のない多剤耐性結核患者に活性化自己T細胞輸注法の効果が期待される。活性化T細胞療法を薬剤抵抗性細菌感染症の新規治療法として確立できれば，長期隔離を余儀なくされている患者の退院が可能となり，患者にとって福音となるばかりでなく医療経済的にも重要な進歩となる。さらに，長期的には薬剤抵抗性細菌感染症の封じ込めに繋がり，社会に対して多大な貢献となるだろう。

## 対象および方法

（A）臨床試験（パイロットスタディー）

平成14年春に東京病院，東京医科歯科大学，国際医療センターからなるプロジェクトチームが結成され，免疫不全症に対する活性化T細胞輸注療法を参考にしつつ，多剤耐性結核患者に対する活性化T細胞輸注療法プロトコールを作成，平成14年10月に東京病院倫理委員会に申請・承認を得た。

その概要は，以下のとおりである。

①フェーズ：院内臨床試験（単施設）

②目的：多剤耐性結核患者を対象に，活性化T細胞輸注療法の安全性と有効性について調べる。

③対象：過去3カ月以上持続排菌している多剤耐性結核患者で，過去6カ月間治療レジメンの変更がない者。

症例1　喀痰塗抹陰性　培養持続陽性の患者

症例2　喀痰塗抹持続陽性の患者

症例3　喀痰塗抹持続陽性，巨大空洞をもつ患者

④用法・用量

試験投与：本治療の前に1/10量の活性化T細胞を点滴静注し，有害事象の発現を調べる。副作用がなければ，本投与を開始する。

本投与：

プロトコール1：$10^9$個の自己活性化Tリンパ球を2週間おきに計6回輸注

プロトコール2：$10^9$個の自己活性化Tリンパ球を4日おきに計3回輸注

2週間あけて同様の輸注を行う。

⑤プリマリーエンドポイントおよび観察項目

リンパ球輸注開始後，3カ月間，培養検査で喀痰中の菌陰性状態が持続するものを有効とする。治療後の有害事象の観察，およびCRP，血沈，ツベルクリン反応，末梢血early secreted antigenic target 6 kDa protein（ESAT-6）刺激下インターフェロンγ産生能（QuantiFERON-TB test）の変化をみる。

（B）CD3-AT法による活性化T細胞の作製

ヘパリン添加末梢血10 mlから比重遠心法にて単核球分離し，抗CD3抗体固相化フラスコ中でIL-2と共に7日間培養し，一部凍結保存し，患者へ投与日より16日前に再度解凍し，抗CD3抗体なしで2日間培養，その後抗CD3抗体固相化フラスコ中でIL-2と共に7日間培養し，ガス透過性バックに移し，抗CD3抗体なしで7日間培養し，細胞を生理食塩水で洗浄後，1% Human Serum Albumin（HSA）加生理食塩水に浮遊，点滴静注する。

（C）*In vitro* 患者活性化T細胞によるBCG殺菌能の検討

多剤耐性結核患者および健常者の末梢血単核球より抗CD3抗体＋IL-2刺激（anti CD3-activated T lymphocyte method：CD3-AT法）により活性化増幅したT細胞を，あらかじめBCG菌を感染させた自己単球由来マクロファージに添加し，殺菌能活性化に必要な細胞数の検討を行った。自己単球由来マクロファージ$1\times10^5$/wellにMOI 1.0の割合でBCG菌を感染させ，2時間後，マクロファージを洗浄し，非感染菌を除去した。直後，$1\times10^5$/wellの割合で自己活性化T細胞または非活性化リンパ球を添加し，4日間培養後，マクロファージ内BCG菌を0.1% Sodium Dodecyl Sulfate/Sodium Buffered Saline（SDS/PBS）で細胞溶解させ，7H10プレートに撒き，培養2～3週間後にコロニーカウントした。

## 結　果

最初に活性化T細胞がマクロファージによる抗酸菌殺菌能を増強させるかどうかを検討した。4人の多剤耐性結核患者および1人の健常者の単球由来マクロファージ内のBCG殺菌実験では，自己活性化T細胞を添加すると添加していないものに比べて$\log_{10}$で2オーダーの殺菌が観察された。非活性化自己リンパ球は全く効果がなかった（図1）。

CD3-AT法により活性化増幅したT細胞を，CD4陽性細胞とCD8陽性細胞に分離し，いずれの細胞が殺菌能を活性化するのかを検討したところ，CD4陽性，CD8陽性細胞ともに分離をしない活性化T細胞に比べて殺菌能は弱かった（data not shown）。このことから，多剤耐性結核患者に対しては，サブセットに分離せず，全T細胞を活性化したものを用いることに決定した。

次に患者に投与する活性化T細胞の表面活性化マーカーのFACS解析では，CD25は，90%以上，CD69は10%程度発現していたが，Interferon-γおよびtumor necrosis factor α（TNF-α）の産生は全くなく，抗CD3抗体による再刺激で産生するようになった。つまり，患者に静注する活性化T細胞はrestingの状態であることが確認された（図2）。

3例の多剤耐性結核患者をプロトコール1に従って治療した。3例ともに輸注中，輸注後に特記すべき有害事象は見られなかった。排菌量の変化であるが，症例1では治療前に喀痰培養持続陽性であったのが，治





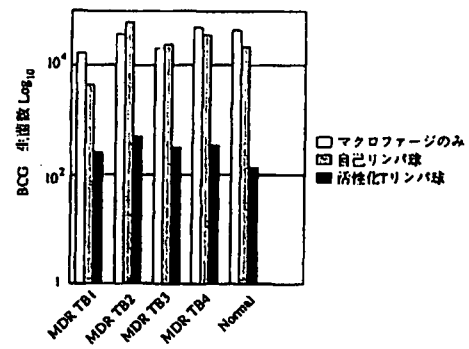


図1　活性化T細胞による自己単球由来マクロファージ内BCG殺菌
MDR：multidrug resistance

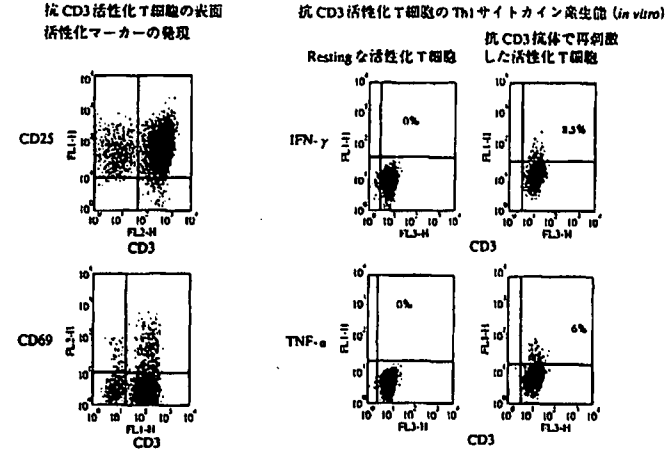


図2　活性化T細胞の表面マーカー発現とサイトカイン産生

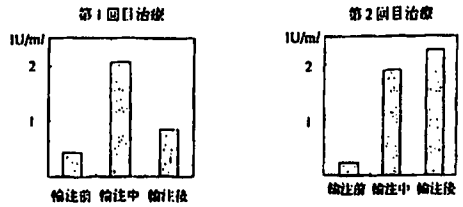


図3 症例2の Quantiferon TB ESAT-6 刺激後末梢血の IFN-γ 産生

療後3カ月間喀痰培養陰性となり，その後再度培養陽性となった。症例2では，喀痰塗抹培養陽性であったが，治療後喀痰塗抹・培養ともに陰性が治療後5カ月間持続し，その後培養陽性となった。症例3に関しては，全く効果なく，排菌量に変化がなかった。症例2については，プロトコール2による再治療を行った。治療後2カ月間培養陰性となったが，再度陽性となっている。

以上の結果をまとめると治療した3例のうち，2例が有効だったが，効果は一時的であった。注目すべきことに，有効であった2例において治療前後のツベルクリン反応 (data not shown) および結核菌 ESAT-6 に対する末梢血のインターフェロンγ産生能が増強されたことである (図3)。

このように，活性化T細胞輸注により，減弱していた結核菌に対する遅延型アレルギー反応が賦活された可能性がある。

## 考　察

本研究は，細胞療法の一種である活性化T細胞輸注療法を難治性の多剤耐性結核の治療へ応用し，化学療法，外科療法に加えて免疫療法も将来取りうる選択肢に加えることを目的としている。今回の検討は，あくまでパイロット的な投与であったが，それでも副作用が認められなかったこと，2例において短期間で一時的であったが，排菌が停止したことは今後の治療法の改良に希望がもてる。これまで，多剤耐性結核に対してはインターロイキン2やインターフェロンγ投与などにより免疫賦活を計る治療法はすでに試みられているが，顕著な効果はでていない。活性化T細胞療法による難治性感染症治療の研究：抗CD3抗体+IL-2刺激 (CD3-AT法) により活性化増幅したT細胞を利用した免疫療法は，がんの免疫治療法として開発され，その治療効果と安全性は無作為抽出試験により証明されている。この治療法のユニークな点は，末梢血T細胞すべてを活性化増幅して投与することであり，特異的T細胞を誘導して治療に用いる方法に比べて，細胞調製が容易であること，様々な抗原に対する効果が期待できるなどの長所がある。

活性化T細胞には *in vitro* においてマクロファージ内のBCG菌殺菌能の増強効果が認められたが，輸注後に活性化T細胞は速やかに組織に移行するといわれており，輸注後のツベルクリン反応の増強や末梢血のESAT-6への反応性の増大は，輸注された活性化T細胞の直接的な作用というよりは，結核菌の慢性感染によるアネルギー状態が解除された結果と考えるほうがよいかもしれない。

今後は，寛解期間を延長するために活性化T細胞の輸注期間を延長したり，他の免疫療法例えば樹状細胞療法と組み合わせるなどの工夫により，本治療の実用化を目指していきたい。







The 79th Annual Meeting Symposium

# STRATEGIES AGAINST MULTIDRUG-RESISTANT TUBERCULOSIS

Chairpersons: [1]Tetsuya TAKASHIMA and [2]Yoshiko KAWABE

**Abstract** Pulmonary tuberculosis can be cured by 6 months chemotherapy, consisting of isoniazid (INH), rifampicin (RFP), pyrazinamide (PZA), and etahanbutol (EB). However, the patients with pulmonary tuberculosis caused by multidrug-resistant tuberculosis (MDR-TB) bacilli, defined as resistance to at least INH and RFP, poorly respond to this regimen. Therefore, the epidemic of MDR-TB in the community is a major threat to tuberculosis control.

According to the interim report of the survey of drug-resistant tuberculosis carried out by Tuberculosis Research Committee Japan in 2002, the prevalence of MDR-TB among new cases, previously treated cases and combined cases was 0.9%, 9.9% and 2.1%, respectively. Thus, the latest Japanese prevalence of MDR-TB was as high as the median prevalence of 72 geographical settings in the world, reported in the WHO/IUATLD Global Project on Drug Resistance Tuberculosis Surveillance, 1994-1999. In Japan, there is still an estimated 2,000 cases of MDR-TB patients. In the last meeting of the Japanese Society for Tuberculosis, an outbreak of MDR-TB in tuberculosis wards was reported, and a careful infection control of MDR-TB was recognized again.

To work out the strategy for the elimination of MDR-TB, two issues were taken up in this symposium. First, not to make new MDR-TB cases, an intervention in the development and spread of MDR-TB was discussed. Second, the effectiveness of conventional anti-tuberculosis chemotherapy and pulmonary resection in the treatment of patients with MDR-TB was reevaluated, and a new approach for the treatment of chronic cases was also discussed.

Dr. Koji Sato (National Amamiwakouen Sanatorium) surveyed the number of patients with MDR-TB in 72 hospitals with tuberculosis wards, and examined the clinical characteristics of chronic cases who had been expecting MDR-TB bacilli in the sputum for more than 5 years. One hundred and twenty-one of 149 chronic cases (81%) in this study were sputum-smear positive. Thirty-seven of them (25%) were outpatients. Thus, the high risk of MDR-TB transmission and the difficulties of infection control of chronic cases were reported.

Dr. Yuka Sasaki (National Hospital Organization Chiba East National Hospital) conducted the questionnaire survey to the ordinance-designated cities and National Sanatoria Hospitals in Japan. Only a few contacts of patients with MDR-TB received preventive treatment, mainly due to the difficulties of diagnosis of latent MDR-TB infections and no effective treatment regimens. She pointed out the importance of preventive treatment guideline for contacts of patients with MDR-TB.

Dr. Masako Wada (Research Institute of Tuberculosis, Japan Anti-Tuberculosis Association) examined the details of acquired MDR-TB cases. Among 2,375 pulmonary tuberculosis patients newly treated in Fukujuji Hospital form 1991 to 2002, 4 cases had developed drug resistance to INH and RFP during treatment. First case was initially INH mono-resistant, which had treated with INH, RFP and EB. Second case had received a sequential mono-therapy after serious adverse reaction. The remaining two cases were supposed to be re-infected with MDR-TB during treatment. This study indicated the importance of improvement of treatment guideline for patients with adverse drug reactions and infection control of MDR-TB in the sanatoria hospitals, in addition to the avoidance of sequential mono-therapy.

Unlike the treatment of drug susceptible tuberculosis, it is not possible to develop a standard treatment regimen for MDR-TB. To know the treatment outcome by the number of susceptible drugs included in each regimen, Dr. Takayuki Nagai (Osaka Prefectural Medical Center for Respiratory and Allergic Diseases) reviewed the 37 patients with pulmonary MDR-TB, knowing the results of susceptibility testing to all 11 anti-tuberculosis drugs, such as INH, RFP, PZA, EB, streptomycin (SM), kanamycin (KM), Enviomycin (EVM), Ethionamide (TH), Cycloserine (CS), Para-aminosalicylic acid (PAS) and levofloxacin (LVFX). Among 11 patients who had received at least 3 susceptible drugs of PZA, LVFX and aminoglycoside, 10 patients (90.9%) had favorable response, converting their sputum cultures to negative at 2 months after the start of chemotherapy. He said that surgical interventions should be considered for any cases, which will not be effectively treated by the regimens including PZA, LVFX and aminoglycoside.

Dr. Yuzo Sagara (National Hospital Organization Tokyo National Hospital) reviewed the surgical outcome of 28 patients with pulmonary MDR-TB with sufficient follow up data. All 8 patients, whose lung lesions had been completely removed, had achieved sputum-culture conversion after surgery and in combination with adequate chemotherapy. Even among 20 patients who still have some lesions after surgery, 14 patients (70.0%) had negative results of sputum cultures. Thus, it is shown that surgical intervention is a major treatment approach to MDR-TB.

Finally, Dr. Koh Nakata (Niigata University Medical Dental Hospital) reported a clinical trial of activated autologous T lymphocytes transfusion to chronic cases. This immunotherapy was well tolerated by all 3 patients. Two patients had responded to this treatment and their sputum culture had become negative for 3-5 months. The host immune up-

regulation was proved by the tuberculin skin test conversion and the increment of IFN-γ production by peripheral blood in response to EAST-6 antigen. It was shown that activated T lymphocyte transfusion might be an effective treatment measure for some chronic cases, by enhancing the host anti-mycobacterial defense systems.

MDR-TB control strategies should be primarily aimed at preventing the emergence of new cases. The rational approach devised by each panelist in this symposium will be the first step to containing the further spread of MDR-TB.

1. Current status of patients with multidrug resistant tuberculosis (MDR-TB) in the long term in Japan: *Koji SATO (National Amamiwakouen Sanatorium), Masashi MORI (National Hospital Organization Tokyo National Hospital)

We surveyed the number of MDR-TB cases in Japan. Four hundreds and eighty-seven cases (4.8%) of 10,208 tuberculosis patients registered in 72 hospitals were MDR-TB. Of them, 149 cases (30.6%) had been expecting MDR-TB bacilli in sputum for a long time more than 5 years. We examined the clinical profiles of these so called chronics. There were 33 females and 116 males. Ninety-eight (65.8%) of them were more than 60 years old. Thirty-seven (24.8%) were out patients. Among 103 cases with the reports of chest X-ray examination, 76 cases (73.8%) had cavity formations. Of them, 24 cases (64.9%) were sputum-smear positive. Difficulties of management and treatment of chronics were recognized again.

2. Chemoprophylaxis for contacts of patients with multidrug-resistant tuberculosis: Yuka SASAKI (Department of Thoracic Disease, National Hospital Organization Chiba East National Hospital)

The chemoprophylaxis to the contacts of patients with multidrug-resistant tuberculosis was considered. The questionnaire survey was conducted to the ordinance-designated cities in Japan. Chemoprophylaxis was performed in 2.4% of contacts of patients with multidrug-resistant tuberculosis, and in the contacts, 20 cases were diagnosed as tuberculosis in the ordinance-designated cities for the past five years. Chemoprophylaxis to the contacts of patients with multidrug-resistant tuberculosis is not carried out positively from many problems in National Sanatoria Hospitals. The present condition is troubled by the correspondence to the contacts of patients with multidrug-resistant tuberculosis.

3. Retrospective examination of treatment failures in newly diagnosed cases, whose strain had acquired multidrug resistance in initial treatment: Masako WADA (Research Institute of Tuberculosis, Japan Anti-Tuberculosis Association)

Not to make a new multidrug resistant tuberculosis case, what should we do for it? First of all, we should treat all new pulmonary tuberculosis cases with 6-month regimen using INH, RFP, EB and PZA, if pyrazinamid is not contraindicated. In this review, two cases of far-advanced multidrug resistant pulmonary tuberculosis patients were presented. One patient received left pneumectomy with chemotherapy of second line anti-tuberculosis drugs, and she had been cured after the completion of 24-month chemotherapy. The other patients died due to massive hemoptysis with chronic respiratory failure at the age of 30 years old. It was supposed the critical different subject to their fates was the timing of reference to a specialist for tuberculosis treatment.

Among 2,608 newly diagnosed pulmonary tuberculosis patients from 1 January 1991 to 31 December 2002, only 4 cases (0.15%) had treatment failures with the emergence of multidrug resistance. First case infected with INH resistant strain was treated with INH, RFP and EB without PZA. Second case complicated with tuberculous pyothorax was also treated with above three drugs regimen. Third case had suffered from a serious skin adverse reaction, and then she had a sequential mono-therapy. The remaining case was suspected to have re-infected with MDR-TB strain.

We should initially treat all pulmonary tuberculosis patients with four drugs regimen. When the treatment failure had occurred due to drug resistant strain, adverse drug reactions or other reasons, it is essential to consult with a specialist for tuberculosis treatment. It should be never done to add anti-tuberculosis drugs one by one to the case of treatment failure.

4. Treatment outcomes of multidrug-resistant tuberculosis: *Takayuki NAGAI, Tetsuya TAKASHIMA, Izuo TSUYUGUCHI (Osaka Prefectural Medical Center for Respiratory and Allergic Diseases)

[Objective] To study the results of anti-tuberculosis chemotherapy of the patients with diagnoses of MDR-TB in our hospital and determine the adequate chemotherapy regimen for MDR-TB.

[Methods] Retrospective study of 37 cases of MDR-TB patients in our hospital between 1999 and 2002. In this study, the five cases were excluded, because they had not received TB treatment for at least 6 months.

[Results] The sputum culture conversion rates at 6 months after starting chemotherapy were 68.8% (22/32). Of them, 2 patients had relapsed bacteriologically during 2 years chemotherapy, 1 patient died, and 2 patients never completed a satisfactory course of treatment. Success rate of treatment was 50.0% (16/32). When 4 or more susceptible drugs were used, treatment success rate was significantly higher than 3 or less drugs were used ($p=0.012$). Among 11 patients who had received at least 3 susceptible drugs of PZA, LVFX and aminoglycoside, 10 patients (90.9%) had favorable response, converting their sputum cultures to negative at 2 months after the start of chemotherapy.

[Conclusion] Surgical interventions should be considered for any cases, which will not be effectively treated by the regimens including PZA, LVFX and aminoglycoside.





5. Surgical management of multidrug resistant pulmonary tuberculosis (MDR-TB): Yuzo SAGARA (National Hospital Organization Tokyo National Hospital)

From January 1991 through December 2002, we operated on 36 MDR-TB patients. Eight complete resections, 23 incomplete resections, and 5 thoracoplasties were performed.

Final success rate of complete resection was 100%. On the other hands, that of incomplete resection was 70%. The cases of MDR-TB within four resistant drugs were successfully treated by incomplete resection.

Complete resection of the pulmonary lesion was the best surgical treatment for MDR-TB, if it is possible.

6. A clinical trial of activated autologous T lymphocytes transfusion for multidrug resistant tuberculosis: *Koh NAKATA*, Emi HAMANO (International Medical Center of Japan, *Bioscience Medical Research Center, Niigata Medical Dental Hospital), Yoshiko KAWABE, Kimihiko MASUDA, Hideaki NAGAI, Haruyuki ARIGA, Atsuyuki KURASHIMA (National Hospital Organization Tokyo National Hospital), Tomohiro MORIO, Norio SHIMIZU (Center for Cell Therapy, Tokyo Medical and Dental University, Medical Hospital)

In multidrug resistant tuberculosis (MDR-TB), T cell function is supposed to be attenuated against *M. tuberculosis*. It is rational to consider that chronic infection lead the host immune system to be anergy state against pathogeons. This study was performed to evaluate the efficacy of activated T lymphocyte transfusion on MDR-TB to reactivate host defense system. One thousand million activated autologous T lymphocytes were transfused every two weeks to three patients with MDR-TB who were chronically positive AFB in their sputum. Two cases responded to this treatment and become negative bacilli in the sputum for 3–5 months, however, they reoccurred afterwards. The other one case did not respond at all. In all three cases, no side effect was observed. Interestingly, in two cases with response, tuberculin skin test and peripheral blood interferon gamma production reacting tuberculosis specific antigen, ESAT-6 were both dramatically augmented during negative bacilli in their sputa. Activated T cell transfusion is safe and may improve the anergy state in some patients with MDR-TB.

Key words: MDR-TB, Case management, Chemoprophylaxis, Treatment

[1]Osaka Prefectural Medical Center for Respiratory and Allergic Diseases, [2]National Hospital Organization Tokyo National Hospital

Correspondence to: Tetsuya Takashima, Osaka Prefectural Medical Center for Respiratory and Allergic Diseases, 3-7-1, Habikino, Habikino-shi, Osaka 583-8588 Japan.
(E-mail: tetsuya@hbk.pref.osaka.jp)

高齢者感染症

# 高齢者の抗酸菌感染症

Mycobacteriosis in elderly

倉島篤行

Key words：結核，非結核性抗酸菌症，高齢者，外来性再感染

## はじめに

抗酸菌感染症は結核症と非結核性抗酸菌症に二分されるが，疾患の伝染性，有病者数，高齢者における高い罹患率，死亡率などで公衆衛生学的には前者が大きな脅威であることはいうまでもない．

しかし，治療において結核症よりはるかに困難な非結核性抗酸菌症はこの数十年で着実に増加し，近年は毎年の新たな抗酸菌陽性患者の約1/3以上を占めると推定され，我が国の非結核性抗酸菌症罹患率は国際的にも有数の高いレベルと推定され今後大きな課題になると考えられる．

## 1. 我が国の高齢者結核の特徴

現在，我が国結核の際立った構造的特徴として高齢者が多いということがいえる[1]．2005年の新登録結核28,319人の中で65歳以上が52.8％を占めている．これは我が国人口構成中での高齢者人口そのものの絶対的増加が主因ではあるが，このような結核登録の年齢階級別分布は世界共通なものではなく，我が国，シンガポール，台湾などかつて結核既感染率が非常に高かった国特有の構造である．

図1は日米の2005年での結核罹患実数を同一の年齢階級別区分で表示したものである．米国の人口は我が国の約2.35倍，2005年の結核罹患率は4.8で我が国よりかなり低いが，図のように実数で比較すると規模の大小がよりわかりやすく興味深い図示となる．44歳以下群では日米の新登録結核は，ほぼ同数であるが，45歳以上群では我が国は圧倒的多数ということがわかる．

今日の高齢者は，第二次世界大戦前後の結核罹患率が人口10万対400を超えるような結核高蔓延時代を生き抜いてきたのであり，高い率で結核菌感染を受け，体内に結核菌が潜伏している．

千葉[2]，Southerland [3]らの研究により，結核は感染を受けた人々の生涯を通して約10-20％に発病し，その5-7割は2年以内に集中するが，残りの発病頻度はなだらかなカーブを描いて漸減すると考えられている．長山によるコーホート分析などで示されるように[4]，高齢者の既感染発病はこの減衰カーブの下で発病するのであり，必ずしも高齢による抵抗力の衰えにより既感染発病率が高齢で上昇するわけではない．これに既発病者の再発病を加えた内因性再燃が今日の高齢者の圧倒的多数を占め，絶対数が多いのはこの母集団である高齢者人口の増加によるものである．しかし，近年RFLP分析などから結核の外来性再感染は少なからずあると考えられるようになった．Jasmerらによれば，米国カナダ地域での結核1,075例を母集団とした再発結核75例のRFLP検討結果では，約4％が外来性再感染と考えられたと報告している[5]．再発結核中での外来性再感染率はその地域での結核罹患率に依存する数字であり，恐らく我が国ではその2-3倍の再感染率が推定される．特に高齢者施設内など特殊な環境では更に高いと考えられる．

以上の群のほか，純粋な新規発病群を加えた，複雑な集団から我が国高齢者結核は形成され，高齢者は現代日本の最大の結核ハイリスクグループとなっている．

我が国人口の高齢化は著しく，65歳以上の高齢者は1998年から2,000万人を超え，2040年には3,380万人に達すると推定されている．長山の近未来予測によれば2018年においても，日本では高齢者結核は大きな問題として存続し続けると推定している．

## 2. 高齢者結核群と他の世代への影響

では高齢者結核群は他の年齢階層への大きな危険因子として影響を及ぼしているだろうか？

井上らは愛知県における1,141人の喀痰塗抹陽性肺結核患者登録から年齢階級別感染源率を解析，報告している[6]．それによれば，感染経路を同じくする複数の発病クラスター中の発端例を感染源とし，二次発病者数に対する割合を感染源率とすると，全年齢では感染源率は6.1％であったが，60歳未満では11.6％，60歳以上では3.3％と有意な差があったとしている．

各種因子についても検討を行っているが，有空洞例が年齢とは独立した感染危険因子であったとしている．従来から高齢者世代から若年者世代への伝搬は想像されるより少ないのではないかということはいわれていたが本報告はそれを裏付けるものであり，著者らはより効率的な高齢者結核対策の提案を行っている．臨床で遭遇する多くの高齢者は，自らが結核高蔓延時代を生き抜いた経歴上，結核伝染に対する自戒の念は現在の中年世代以下群よりはるかに意識的，自制的な場合が多く，一つはこのような自覚に伴う行動様式の反映かもしれない．

## 3. 高齢者結核臨床像の特徴と問題点

高齢者結核臨床像の特徴として既に多くの報告やメタアナリシス[7]で，合併症数が多く結核死亡率も高い，自覚症に乏しく画像所見でも有空洞型は他の世代群に比べ有意に少ないなどが述べられている．我が国の結核検診では伝統的に胸部X線診断が重視されてきたが，高齢者結

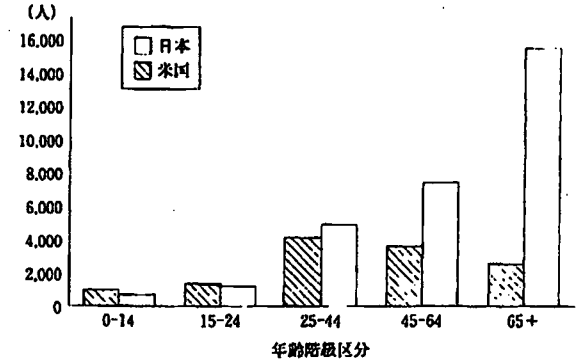


図1　2005年，日米年齢階級区分別新登録結核実数
（結核の統計2006（厚生労働省健康局結核感染症課監修）と米国CDC結核疫学調査報告より作図）

Atsuyuki Kurashima: Division of Clinical Research, National Hospital Organization Tokyo Hospital　独立行政法人国立病院機構東京病院　臨床研究部

0047-1852/07/¥40/頁/JCLS

Available online at www.sciencedirect.com
ScienceDirect
Journal of Microbiological Methods 72 (2008) 149–156
Journal of Microbiological Methods
www.elsevier.com/locate/jmicmeth

# Comprehensive analysis of mycolic acid subclass and molecular species composition of *Mycobacterium bovis* BCG Tokyo 172 cell wall skeleton (SMP-105)

Yuko Uenishi [a,*], Yukiko Fujita [b], Naoto Kusunose [c], Ikuya Yano [b], Makoto Sunagawa [d]

[a] *Technology Research & Development Center, Dainippon Sumitomo Pharma Co., Ltd., 1-3-45, Kurakakiuchi, Ibaraki-shi, Osaka 567-0878, Japan*
[b] *Japan BCG Central Laboratory, 3-1-5 Matsuyama, Kiyose-shi, Tokyo 204-0022, Japan*
[c] *Drug Research Division, Dainippon Sumitomo Pharma Co., Ltd., 3-1-98, Kasugade-naka, Konohana-ku, Osaka-shi, Osaka 554-0022, Japan*
[d] *Faculty of Pharmaceutical Sciences, Teikyo Heisei University, 2289-23, Uruido, Ichihara-shi, Chiba 290-0193, Japan*

Received 16 April 2007; received in revised form 21 October 2007; accepted 13 November 2007
Available online 22 November 2007

**Abstract**

The mycobacterial cell envelope consists of a characteristic cell wall skeleton (CWS), a mycoloyl arabinogalactan peptidoglycan complex, and related hydrophobic components that contribute to the cell surface properties. Since mycolic acids have recently been reported to play crucial roles in host immune response, detailed molecular characterization of mycolic acid subclasses and sub-subclasses of CWS from *Mycobacterium bovis* BCG Tokyo 172 (SMP-105) was performed. Mycolic acids were liberated by alkali hydrolysis from SMP-105, and their methyl esters were separated by silica gel TLC into three subclasses: α-, methoxy-, and keto-mycolates. Each mycolate subclass was further separated by silver nitrate ($AgNO_3$)-coated silica gel TLC into sub-subclasses. Molecular weights of individual mycolic acid were determined by MALDI-TOF mass spectrometry. α-Mycolates were sub-grouped into *cis*, *cis*-dicyclopropanoic (α1), and *cis*-monocyclopropanoic-*cis*-monoenoic (α2) series; methoxy-mycolates were sub-grouped into *cis*-monocyclopropanoic (m1), *trans*-monocyclopropanoic (m2), *trans*-monoenoic (m3), *cis*-monocyclopropanoic-*trans*-monoenoic (m4), *cis*-monoenoic (m5), and *cis*-monocyclopropanoic-*cis*-monoenoic (m6) series; and keto-mycolates were sub-grouped into *cis*-monocyclopropanoic (k1), *trans*-monocyclopropanoic (k2), *trans*-monoenoic (k3), *cis*-monoenoic (k4), and *cis*-monocyclopropanoic-*cis*-monoenoic (k5) series. The position of each functional group, including cyclopropane rings and methoxy and keto groups, was determined by analysis of the meromycolates with fast atom bombardment (FAB) mass spectrometry and FAB mass-mass spectrometry, and the *cis*/*trans* ratio of cyclopropane rings and double bonds were determined by NMR analysis of methyl mycolates. Mycolic acid subclass and molecular species composition of SMP-105 showed characteristic features including newly-identified *cis*-monocyclopropanoic-*trans*-monoenoic mycolic acid (m4).


*Keywords:* Mycolic acids; BCG-CWS; SMP-105; *M. bovis* BCG Tokyo 172

## 1. Introduction

The mycobacterial cell envelope consists of numerous high molecular weight lipid components, most of which induce diverse host immune responses (Beckman et al., 1994). The cell wall skeleton (CWS) is unique and ubiquitous; however, the fine structure consisting of mycoloyl arabinogalactan-peptidoglycan complex (McNeil et al., 1991; Brennan and Nikaido, 1995; McNeil, 1999; Brennan, 2003) differs among species of mycobacteria. Recently, CWS of *Mycobacterium bovis* BCG has been reported to be a potent anti-cancer immunotherapeutic, based on the host-anti tumor immune response (Seya et al., 2001; Yoo et al., 2002; Akazawa et al., 2004; Nakajima et al., 2004). However, BCG-CWS is a very large hetero lipoglycan containing mycolic acids, which are very long branched-chain hydroxy fatty acids. The structure-biological activity relationship of BCG-CWS has not been fully established, although analytical studies and anti-tumor therapeutic investigations were started 30 years ago (Azuma et al., 1974; Yamamura et al., 1976a,b; Yasumoto et al., 1976; Nishikawa et al., 1978;

* Corresponding author. Tel.: +81 72 627 8214; fax: +81 72 627 8140.
*E-mail address:* yuko-uenishi@ds-pharma.co.jp (Y. Uenishi).

0167-7012/$ - see front matter © 2007 Elsevier B.V. All rights reserved.
doi:10.1016/j.mimet.2007.11.016

Yamamura et al., 1979; Yasumoto et al., 1979; Hayashi et al., 1998; Tsuji et al., 2000; Azuma and Seya, 2001; Matsumoto et al., 2001; Begum et al., 2004; Ishii et al., 2005).

Recent studies reported that BCG-CWS shows potent adjuvant activity via Toll-like receptors (TLR)-2 and-4 as a pathogen-associated molecular pattern (PAMP) for host animal immune systems, and both mycolic acids and peptidoglycan moieties play central roles in the expression of such activities in experimental animal systems (Seya et al., 2001; Yoo et al., 2002; Akazawa et al., 2004; Nakajima et al., 2004). Recently, mycolic acids have been reported to be CD-1 restrictive lipid antigens presented by dendritic cells (Beckman et al., 1994), and therefore detailed structure analysis of mycolic acids is required. In the present study, we introduced modern techniques for comprehensive analysis of mycolic acids of BCG-CWS. The structure of each subclass and molecular species of mycolic acids was analyzed on the highly purified CWS from *M. bovis* BCG Tokyo 172 (hereafter called SMP-105) after proteinase digestion, DNAase treatment, and delipidation with organic solvents of crude cell wall preparations. Although cellular mycolic acid composition of *M. bovis* BCG substrains were reported in some detail previously (Minnikin et al., 1984; Kaneda et al., 1986, 1988, 1995; Watanabe et al., 2001, 2002; Fujita et al., 2005a,b), the present paper is the first to describe analytical results of fully-separated mycolic acid subclasses and molecular species of *M. bovis* BCG Tokyo cell wall skeleton (SMP-105).

## 2. Methods

### 2.1. Bacterial strain and growth conditions

*M. bovis* BCG Tokyo 172 was grown at 37 °C on the surface of Sauton medium for 9 days. The bacterial culture was heated at 80 °C for 30 min to inactivate the cells, and then centrifuged.

### 2.2. Preparation of SMP-105

SMP-105 was prepared from crude cell wall preparation of heat-killed *M. bovis* BCG Tokyo 172, essentially in accordance with a method reported previously (Azuma et al., 1974; Uenishi et al., 2007). Briefly, the heat-inactivated bacterial cells were disrupted with Mini DeBEE (BEE International) at 35 kpsi. The disrupted cells were centrifuged at 6760 ×*g* first to remove large debris and undisrupted cells, and then centrifuged again at 18,000 ×*g* to obtain pellet of whole cell wall (WCW). WCW was incubated with benzonase (Merck) at 25 °C for 17 h, followed by pronase (Sigma-Aldrich) at 37 °C for 17 h to digest nucleic acids and proteins, respectively. The enzyme-digested cell walls were washed with 1% polyoxyethylene (10) octylphenyl ether (Triton X-100), then treated with ethanol, tetrahydrofuran, chloroform, and methanol consecutively to remove lipids, and finally dried to obtain SMP-105.

### 2.3. Preparation of mycolic acid methyl esters by silica gel TLC

The SMP-105 thus obtained was treated with 0.5 M potassium hydroxide/toluene/ethanol (10:10:1, v/v/v) at 65 °C for 3 h, followed by acidification with diluted hydrochloric acid, and then the mycolic acids were extracted with n-hexane. Crude mycolic acids were methylated with 10% trimethylsilyldiazomethane in *n*-hexane (Nacalai Tesque) for more than 30 min at room temperature. Mycolic acid methyl esters were separated by HPTLC (Silica gel 60, 10 × 10 cm, Merck) and developed with a solvent of n-hexane/ethyl acetate (20:1, v/v) three times. Methyl esters, separated into α-, methoxy-, and keto-mycolates, were extracted from silica gel TLC with chloroform/methanol (4:1, v/v).

### 2.4. Separation of mycolic acid methyl esters by $AgNO_3$-coated silica gel TLC

Silver nitrate ($AgNO_3$)-coated silica gel plates were prepared for HPTLC (Silica gel 60, 10 × 10 cm, Merck) with a 10% solution of $AgNO_3$ in acetonitrile, followed by drying. Each α-, methoxy-, and keto-mycolate was applied to $AgNO_3$-coated silica gel TLC and separated into two or three spots (described below) with *n*-hexane/ethyl acetate (20:1, v/v) as a solvent system. After visualizing by spraying with water, the sub-subclass mycolic acid methyl esters were recovered from $AgNO_3$-coated silica gel TLC with chloroform and methanol. The amount of each mycolate recovered was determined by weight.

### 2.5. Mass spectrometric analysis of mycolic acid subclasses

The molecular weight of each mycolic acid methyl ester was determined by MALDI-TOF mass spectrometry on Voyager DE-STR (Applied Biosystems) using 2,5-dihydroxybenzoic acid (2,5-DHB) as a matrix, as reported previously (Laval et al., 2001; Fujita et al., 2005a,b). The positions of cyclopropane rings, and methoxy and keto groups were determined by FAB mass (JEOL JMS-SX102) and FAB mass-mass (JEOL JMS-HX/HX 110A) analyses of methyl meromycolates. The methyl meromycolates were prepared as follows: Mycolic acid methyl ester of each subclass was dissolved in acetone/n-hexane (4:1, v/v) and the hydroxyl group was oxidized with Jones reagent (Bowden et al., 1946; Heilbron et al., 1949) at room temperature for 1 h. The resultant β-keto-ester was extracted with n-hexane. After evaporating the solvent, the residues were dissolved in dehydrated methanol/dehydrated tetrahydrofuran (1:1, v/v) and then treated with sodium methoxide at 50 °C for 3 h. After full methylation, samples were neutralized with 2 M hydrochloric acid, and then extracted with *n*-hexane. The resultant meromycolic acid methyl esters were detected by silica gel TLC, and then extracted with chloroform and methanol. The isolated meromycolic acid methyl esters, having different polar groups in the alkyl chain, were mixed with n-nitrobenzyl alcohol and LiI as a matrix, and applied to FAB mass and FAB mass-mass analyses to determine the positions of the functional groups.

### 2.6. $^1H$ NMR analysis of mycolic acid subclasses

$^1H$ NMR (500 MHz) spectra of each mycolic acid subclasses were recorded on a JEOL A-500 spectrometer and chemical shifts were referred to internal $CDCl_3$ (7.24 ppm).

## 3. Results

### 3.1. Separation of mycolic acid methyl esters by silica gel TLC

Total mycolic acid methyl esters from SMP-105 were separated into α-, methoxy-, and keto-mycolates by silica gel TLC. The relative amount of each mycolic acid methyl ester subclass recovered from SMP-105 was approximately 17:17:66 w/w/w (Suppl. Fig. 1(a)).

Next, to reveal the detailed molecular species composition, each subclass of mycolic acid methyl ester was further separated by $AgNO_3$-coated silica gel TLC, according to the degree of unsaturation. As a result, α-mycolic acid methyl esters were separated into two major spots (Suppl. Fig. 1(b); spots 2 and 3), and methoxy-and keto-mycolic acid methyl esters were separated into three major spots (Suppl. Fig. 1(b); spots 5, 6, 7 and 9, 10, 11). Each spot was recovered from $AgNO_3$-coated silica gel TLC and subjected to MALDI/TOF mass spectrometry. On $AgNO_3$-coated silica gel TLC, saturated, *trans*-monoenoic and *cis*-monoenoic mycolic acid methyl esters were clearly separated, but separation of *cis*-or *trans*-cyclopropanoic mycolates was unsuccessful. The relative yield of each sub-subclass mycolic acid was as follows: α-mycolate, upper spot 51% and lower spot 3%; methoxy-mycolate, uppermost spot 84%, middle spot 3%, and lowest spot 2%; and keto-mycolate, uppermost spot 78%, middle spot 2% and lowest spot 1%, by weight.

### 3.2. Identification of mycolic acid methyl ester subclasses and molecular species by MALDI-TOF mass analysis

MALDI-TOF mass spectra of mycolic acid methyl esters from SMP-105 showed major clusters of mass ions due to $[M+Na]^+$ (where M is the molecular mass of the mycolic acid methyl ester sub-subclass). We analyzed each molecular species of methyl mycolate sub-subclass separated by $AgNO_3$-coated silica gel TLC and summarized the MALDI-TOF mass spectrometry data of these mycolic acid types in Table 1.

α-Mycolates are the principal mycolic acid subclass in all mycobacterial species. By $AgNO_3$-coated silica gel TLC, α-mycolic acid methyl esters were further separated into two spots (α1 and α2). Positive MALDI-TOF mass spectra of α1 mycolate from $AgNO_3$-coated silica gel TLC showed distinctively the most abundant mass ion at *m/z* 1173, due to $C_{78}$ α-mycolate with two *cis*-cyclopropane rings (Suppl. Fig. 2(a)). Molecular mass ions due to $C_{74}$, $C_{76}$, $C_{80}$, and $C_{82}$ α-mycolates were also clearly demonstrated. While mass spectra of α2 spot showed the most abundant ion at *m/z* 1159, due to $C_{77}$ α-mycolate with one *cis*-cyclopropane ring and one *cis*-double bond, mass ions due to $C_{75}$, $C_{79}$, and $C_{81}$ α-mycolates were also detected (Suppl. Fig. 2(b)). It was revealed that the α1 series of α-mycolates comprised even carbon-numbered mycolates with two *cis*-cyclopropane rings, while the α2 series comprised odd carbon-numbered mycolates with one *cis*-cyclopropane ring and one *cis*-double bond, exclusively. It was also noted that a small but significant amount of ions due to $C_{72}$ (*m/z* 1091), $C_{74}$ (*m/z* 1119), and $C_{76}$ (*m/z* 1147) shorter-chain monoenoic even carbon-numbered α-mycolates were observed in the TOF mass spectrum (Suppl. Fig. 2(b)).

Methoxy-mycolates are a characteristic polar mycolic acid subclass in *M. tuberculosis* complex and *M. bovis* BCG Tokyo 172, but are lacking in some *M. bovis* BCG substrains (Minnikin et al., 1984; Watanabe et al., 2002). The MALDI-TOF mass spectra of uppermost spot of the methoxy-mycolate sub-subclass showed the most abundant ion at *m/z* 1289, due to $C_{85}$ *cis*-monocyclopropanoic methoxy-mycolates, with small amounts of $C_{81}$, $C_{83}$, $C_{87}$, and $C_{89}$ homologues (m1) (Suppl. Fig. 3(a)). This group also contained small amounts of longer-chain even carbon-numbered homologues with centering at $C_{84}$, $C_{86}$, and $C_{88}$, due to *trans*-cyclopropanoic methoxy-mycolate (m2), while the mass spectra of middle spot of the methoxy-mycolate sub-subclass also showed the most abundant ion at *m/*

Table 1
MALDI-TOF mass spectrometry data of mycolic acid sub-subclasses of CWS from *M. bovis* BCG Tokyo 172 (SMP-105)

| Mycolic acid type | Sub-sub class | Position on $AgNO_3$ TLC | Total number of carbons in mycolic acid | | | | | | | | | | | | | | | |
|---|---|---|---|---|---|---|---|---|---|---|---|---|---|---|---|---|---|---|
| | | | 74 | 75 | 76 | 77 | 78 | 79 | 80 | 81 | 82 | 83 | 84 | 85 | 86 | 87 | 88 | 89 |
| α | α1 | 2 | 1117 | | 1145 | | 1173 | | 1201 | | 1229 | | | | | | | |
| | α2 | 3 | | **1131** | | **1159** | | **1187** | | 1215 | | | | | | | | |
| **Methoxy** | m1 | 5 | | | | | | | | 1233 | | **1261** | | **1289** | | **1317** | | 1345 |
| | m2 | | | | | | | | | | | | 1275 | | 1303 | | 1331 | |
| | m3 | 6 | | | | | | | | 1233 | | **1261** | | **1289** | | 1317 | | |
| | m4 | | | | | | | | 1217 | | 1245 | | 1273 | | 1301 | | 1329 | |
| | m5 | 7 | | | | | | | | 1233 | **1247** | 1261 | **1275** | 1289 | 1303 | | 1331 | 1345 |
| | m6 | | | | | | | | | | | 1259 | | 1287 | | 1315 | | 1343 |
| **Keto** | k1 | 9 | | | | | | | 1217 | | **1245** | | **1273** | | **1301** | | 1329 | |
| | k2 | | | | | | | | | | | 1259 | | 1287 | | **1315** | | 1343 |
| | k3 | 10 | | | | | | | 1217 | | **1245** | | **1273** | | 1301 | | | |
| | k4 | 11 | | | | | | 1203 | | **1231** | | **1259** | | 1287 | | 1315 | | |
| | k5 | | | | | | | | | | | | 1271 | | 1299 | | 1327 | |

Values represent the pseudomolecular mass $[M+Na]^+$ of methyl mycolate. Subtypes of mycolic acids are α1, *cis*, *cis*-dicyclopropanoic; α2, *cis*-monocyclopropanoic-*cis*-monoenoic; m1, *cis*-monocyclopropanoic methoxy; m2, *trans*-monocyclopropanoic methoxy; m3, *trans*-monoenoic methoxy; m4, *cis*-monocyclopropanoic-*trans*-monoenoic methoxy; m5, *cis*-monoenoic methoxy; m6, *cis*-monocyclopropanoic-*cis*-monoenoic methoxy; k1, *cis*-monocyclopropanoic keto; k2, *trans*-monocyclopropanoic keto; k3, *trans*-monoenoic keto; k4, *cis*-monoenoic keto; and k5, *cis*-monocyclopropanoic-*cis*-monoenoic keto mycolic acids. Major homologues are shown in bold.

z 1289, due to $C_{85}$ monoenoic methoxy-mycolate, with smaller amounts of $C_{81}$, $C_{83}$, and $C_{87}$ homologues (m3) (Suppl. Fig. 3 (b)). Furthermore, in this subgroup, small but significant amounts of ions due to even carbon-numbered diene-equivalent methoxy-mycolates were observed, centering at $C_{84}$ and ranging from $C_{80}$ to $C_{88}$ (m4). Judging from the chromatographic behaviors and mass numbers, the former (m3) should be *trans*-monoenoic methoxy-mycolate exclusively, while the latter (m4) should be *cis*-monocyclopropanoic-*trans*-monoenoic methoxy-mycolate, as yet not reported in *M. bovis* BCG. The mass spectra of lowest spot of the methoxy-mycolate sub-subclass showed the most abundant ion at *m/z* 1275, due to $C_{84}$ *cis*-monoenoic methoxy-mycolate, with smaller amounts of $C_{81}$ to $C_{89}$ homologues (m5) (Suppl. Fig. 3(c)). Furthermore, also in this subgroup, small but significant amounts of ions due to odd carbon-numbered diene-equivalent methoxy-mycolates were observed, centering at $C_{87}$ and ranging from $C_{83}$ to $C_{89}$ (m6). Judging from the chromatographic behaviors and mass numbers, the former (m5) should be *cis*-monoenoic methoxy-mycolate, while the latter (m6) should be *cis*-monocyclopropanoic-*cis*-monoenoic methoxy-mycolate, exclusively.

Keto-mycolates are another of the major mycolate subclasses, distributed widely among rapid-and slow-growing mycobacteria. The MALDI-TOF mass spectra of uppermost spot of the keto-mycolate sub-subclass showed the most abundant ion at *m/z* 1273, due to $C_{84}$ monocyclopropanoic keto-mycolate, with smaller amounts of $C_{80}$, $C_{82}$, $C_{86}$, and $C_{88}$ even carbon-numbered homologues (k1) (Suppl. Fig. 4(a)). Furthermore, in this series, substantial amounts of ions due to longer chain odd carbon-numbered monoene-equivalent keto-mycolates were observed, centering at $C_{87}$ and ranging from $C_{83}$ to $C_{89}$ (k2). Judging from the chromatographic behaviors and mass numbers, the former (k1) should be *cis*-monocyclopropanoic keto-mycolates, while the latter (k2) should be *trans*-monocyclopropanoic keto-mycolates, exclusively. The mass spectra of middle spot of the keto-mycolate sub-subclass also showed the most abundant ion at *m/z* 1273, due to $C_{84}$ monoenoic keto-mycolate with smaller amounts of $C_{80}$, $C_{82}$, and $C_{86}$ homologues (k3) (Suppl. Fig. 4(b)). Based on the chromatographic behaviors, k3 possesses one *trans*-double bond, exclusively. The mass spectra of lowest spot of the keto-mycolate sub-subclass showed the most abundant ion at *m/z* 1259, due to $C_{83}$ monoenoic keto-mycolate with smaller amounts of $C_{79}$, $C_{81}$, $C_{85}$, and $C_{87}$ homologues (k4) (Suppl. Fig. 4(c)). Furthermore, also in this sub-subgroup, small but significant amounts of ions due to longer chain even carbon-numbered diene equivalent keto-mycolates were observed, centering at $C_{86}$ and ranging from $C_{84}$ to $C_{88}$ (k5). Judging from the chromatographic behaviors and mass numbers, the former (k4) should be *cis*-monoenoic keto-mycolates, while the latter (k5) should be *cis*-monocyclopropanoic-*cis*-monoenoic keto-mycolates.

### 3.3. Determination of the location of functional groups of mycolic acid sub-subclasses by FAB mass-mass analysis

To determine the locations of the functional groups of mycolic acids from SMP-105, meromycolic acid methyl esters were prepared and analyzed by FAB mass-mass analysis. Methyl meromycolates were prepared by a facile method, different from the pyrolysis reported by Watanabe et al. (2002): Jones oxidation of each methyl mycolate and the following retro-Dieckmann reaction yielded the desired methyl meromycolates (Suppl. Fig. 5). In the present study, the locations of *cis*- and *trans*-double bonds, *cis*-and *trans*-cyclopropane rings, methoxy and keto groups, and methyl branches adjacent to the methoxy or keto groups were determined based on the characteristic bond-cleavage profiles (Tomer et al., 1986; Cheng and Gross, 1998). Functional groups nearer to the carboxyl group are referred to as "proximal," whereas the others are referred to as "distal," for convenience.

FAB mass spectra of α-meromycolates from upper spot showed one major and one minor peak due to the molecular ions at *m/z* 777 and 805, respectively. A mass ion at *m/z* 777, corresponding to the meromycolate derived from $C_{78}$ α-mycolate with two *cis*-cyclopropane rings (α1), the most abundant α-mycolate species, was further decomposed by FAB mass-mass spectroscopy, and the prominent ions due to cleavages at the β-position of the distal and proximal cyclopropane rings were detected (Suppl. Fig. 6(a)). As a result, the position of the distal cyclopropane ring of $C_{52}$ α-meromycolate derived from $C_{78}$ *cis*, *cis*-dicyclopropanoic α-mycolate was shown to be located at the 21st position from the omega end of the alkyl chain, while that of the proximal ring was considered to be at the 13th position from the carboxyl end, exclusively. Similarly, in the case of other dicyclopropanoyl α-mycolates, the distal *cis*-cyclopropane ring was consistently located at the 21st position from the omega end of the meromycolate chain, while the location of the proximal ring was variable according to the chain length of meromycolates. The location of the *cis*-, but not *trans*-double bond, of monocyclopropanoic monoenoic α-mycolate sub-subclass (α2) is most likely identical to those of the corresponding di-*cis*-cyclopropane rings. Most of the analytical data obtained above agreed with those reported previously (Watanabe et al., 2002), although quantitative results differed.

FAB mass spectra of methoxy-meromycolates from upper spot showed five or more peaks due to multi sub-subclasses and molecular species, among which ions at *m/z* 865, 893, and 921 were further decomposed by FAB mass-mass spectroscopy. The mass-mass spectrum of the ion at 893, due to $C_{59}$ methoxy-meromycolate derived from $C_{85}$ methoxy-mycolate with a monocyclopropane ring, mono methyl branch, and methoxy function (m1) (Suppl. Fig. 6(b)). The results showed a characteristic ion at *m/z* 597, due to the cleavage between each pair of carbon units having a methyl branch and methoxy function, and the loss of the methyl group from the latter. With the ion at *m/z* 609, due to the α-cleavage to methyl branch and the loss of the O-methyl group, the location of the methyl branch was identified to be at the 19th position from the omega end, and that of the adjacent methoxy group was judged to be at the 20th position, exclusively. Furthermore, since this molecular species was suggested to possess one cyclopropane ring at the proximal position, the location was again identified based on the β-cleavage at both sides of the ring. The results showed prominent ions at *m/z* 289 and 357, indicating the *cis*-cyclopropane ring was located at the 19th position from the

carboxyl end of the meromycolate. The locations of the functional groups of meromycolates belonging to other series were determined similarly. The locations of the methyl branch and O-methyl groups from the omega end of meromycolates were essentially the same among all the methoxy-mycolic acid sub-subclasses, while those of other proximal functional groups such as *cis*-or *trans*-cyclopropane rings, or *cis*-and *trans*-double bonds differed according to the chain length of the meromycolate, reflecting the biosynthetic mechanism and introduction rule of functional groups into meromycolic acids. It was particularly noted that the methoxy-mycolic acid sub-subclass was composed mainly of odd carbon-numbered *trans*-monoenoic methoxy-mycolate (m3), and further, the same methoxy-mycolate subclass showed substantial intensity of mass ions due to even carbon-numbered diene-equivalent subspecies (m4), centering at $C_{84}$ and ranging from $C_{80}$ to $C_{88}$. Although such diene-equivalent series of even carbon-numbered methoxy-mycolates has not been reported in *M. bovis* BCG substrains, these molecular species or subclasses seemed most likely to be *cis*-monocyclopropanoic-*trans*-monoenoic methoxy-meromycolates. These results were confirmed by NMR analysis.

FAB mass spectra of keto-meromycolates from upper spot showed ten or more peaks due to diverse subclasses and molecular species composition, among which ions at *m/z* 877, 905, and 919 were further decomposed by FAB mass-mass spectroscopy. The mass-mass spectrum of the ion at 877, due to $C_{58}$ keto-meromycolic acid derived from $C_{84}$ keto-mycolate (k1) with a monocyclopropane ring, monomethyl branch, and carbonyl functions (Suppl. Fig. 6(c)). The results showed characteristic ions at *m/z* 553 and 637, due to the β-cleavages of both sides of two functional groups ($-CH_2-CO-CH(CH_3)-CH_2-$). These fragmentations indicate the existence of a methyl group and an adjacent carbonyl group at the 19th position from the omega end, and therefore the 37th position of the carboxy end of meromycolate, exclusively. Furthermore, since this molecular species was suggested to possess one cyclopropane ring at the proximal position, the location was again identified based on the β-cleavage at both sides of the ring. The results showed the ions at *m/z* 289 and 357, indicating the proximal *cis*-cyclopropane ring was probably located at the 19th position from the carboxyl end of the meromycolate. The locations of the functional groups of keto-meromycolates belonging to other series were determined similarly.

### 3.4. $^1H$ NMR analysis of mycolic acid subclasses

$^1H$ NMR spectra of α-, methoxy-, and keto-mycolates, each major spot obtained by $AgNO_3$-coated silica gel TLC, were recorded and shift values were measured in ppm (δ) relative to internal $CHCl_3$. An $^1H$ NMR spectrum (Suppl. Fig. 7(a)) of the most abundant subclass α1-mycolates with two cyclopropane rings, showing common signals of mycolic acid methyl esters, such as those due to $-(CH_2)_nCH_3$,$-CH_2(CH_2)_nCH_2-$,$-CH_2CH(OH)-$,$-CH_2CH(COOCH_3)-$,$-CH(COOCH_3)-$,$-CH(OH)-$, and $-COOCH_3$, as well as α1 subclass-specific signals, such as those due to *cis*-cyclopropane rings at around δ 0.53 to 0.62 and δ −0.36. An $^1H$ NMR spectrum (Suppl. Fig. 7(b)) of the most abundant subclass methoxy-mycolates including m1 and m2 with one *cis*-or *trans*-cyclopropane ring, showing methoxy-mycolic acid methyl ester-specific signals, such as those due to $-CHOCH_3$ at δ 3.30 with a *cis*-cyclopropane ring. An $^1H$ NMR spectrum (Suppl. Fig. 7(c)) of the most abundant keto-subclass mycolates including k1 and k2 with one cyclopropane ring including both *cis*-and *trans*-configurations. All $^1H$ NMR parameters for each of these mycolic acid subclasses are listed in Table 2. Based on the combined results obtained from mass spectrometric analyses (MALDI-TOF mass and FAB mass) and $^1H$ NMR parameters, it was concluded that α-mycolates (α1 and α2) contained one or two *cis*-cyclopropane ring(s) but did not contain *trans*-cyclopropane rings; methoxy-mycolates (m1 and m2) contained one cyclopropane ring with *cis*-or *trans*-configurations in which the *cis*-form predominated; and keto-mycolates (k1 and k2) also contained one cyclopropane ring with *cis*-or *trans*-configurations in which the *cis*-form predominated, but more *trans*-form existed than in the case of methoxy-mycolates. The *cis*-to *trans*-form ratios in methoxy- and keto-mycolates were calculated using the accumulated

Table 2
$^1H$ NMR signals characteristic of methyl mycolate subclasses of CWS from *M. bovis* BCG Tokyo 172 (SMP-105)

| Mycolic acid type | Sub-sub class | Position on $AgNO_3$ TLC | Δ | $-CHCH_3$ | $-CHOR$ | $-CHOCH_3$ | *cis*/trans |
|---|---|---|---|---|---|---|---|
| α | α1 | 2 | −0.36 (m, 1H) cis<br>0.53 (m, 1H) cis<br>0.62 (m, 2H) cis | | | | 100:0 |
| Methoxy | m1 and m2 | 5 | −0.36 (m, 1H) cis<br>0.53 (m, 1H) cis<br>0.62 (m, 2H) cis<br>0.04 to 0.19 (m, 3H) trans<br>0.42 (m, 1H) trans | 0.85 (d, 3H) | 2.93 (m, 1H) | 3.30 (s, 3H) | 91:9 |
| Keto | k1 and k2 | 9 | −0.36 (m, 1H) cis<br>0.53 (m, 1H) cis<br>0.62 (m, 2H) cis<br>0.04 to 0.19 (m, 3H) trans<br>0.42 (m, 1H) trans | 0.85 (d, 3H) | – | – | 71:29 |

Common signals to all mycolic acid methyl esters: δ 0.86 ($-(CH_2)_nCH_3$, t, 6H), δ 1.0–1.5 ($-CH_2(CH_2)_nCH_2-$, br, m), δ 1.54 ($-CH_2CH(OH)-$, m, 2H), δ 1.66 ($-CH_2CH(CO_2CH_3)-$, m, 2H), δ 2.40 ($-CH(CO_2CH_3)-$, m, 1H), δ 3.62 ($-CH(OH)-$, br, m, 1H), δ 3.68 ($(-CO_2CH_3)-$, s, 3H).
br; broad, s; singlet, d; doublet, t; triplet, m; multiplet.

intensity of peaks attributable to the *cis*-form observed at around $\delta$ 0.53 to 0.62 and $\delta$ −0.36, and that of peaks attributable to *trans*-form at around $\delta$ 0.42 and $\delta$ 0.04 to 0.19. As a result, it was concluded that the ratio of *cis*- to *trans*-form of cyclopropane rings of methoxy-mycolates (m1 and m2) was 91:9 and that of keto-mycolates (k1 and k2) was 71:29.

As described above, among the three subclasses of mycolic acids, six sub-subclasses of methoxy-mycolates were specific to

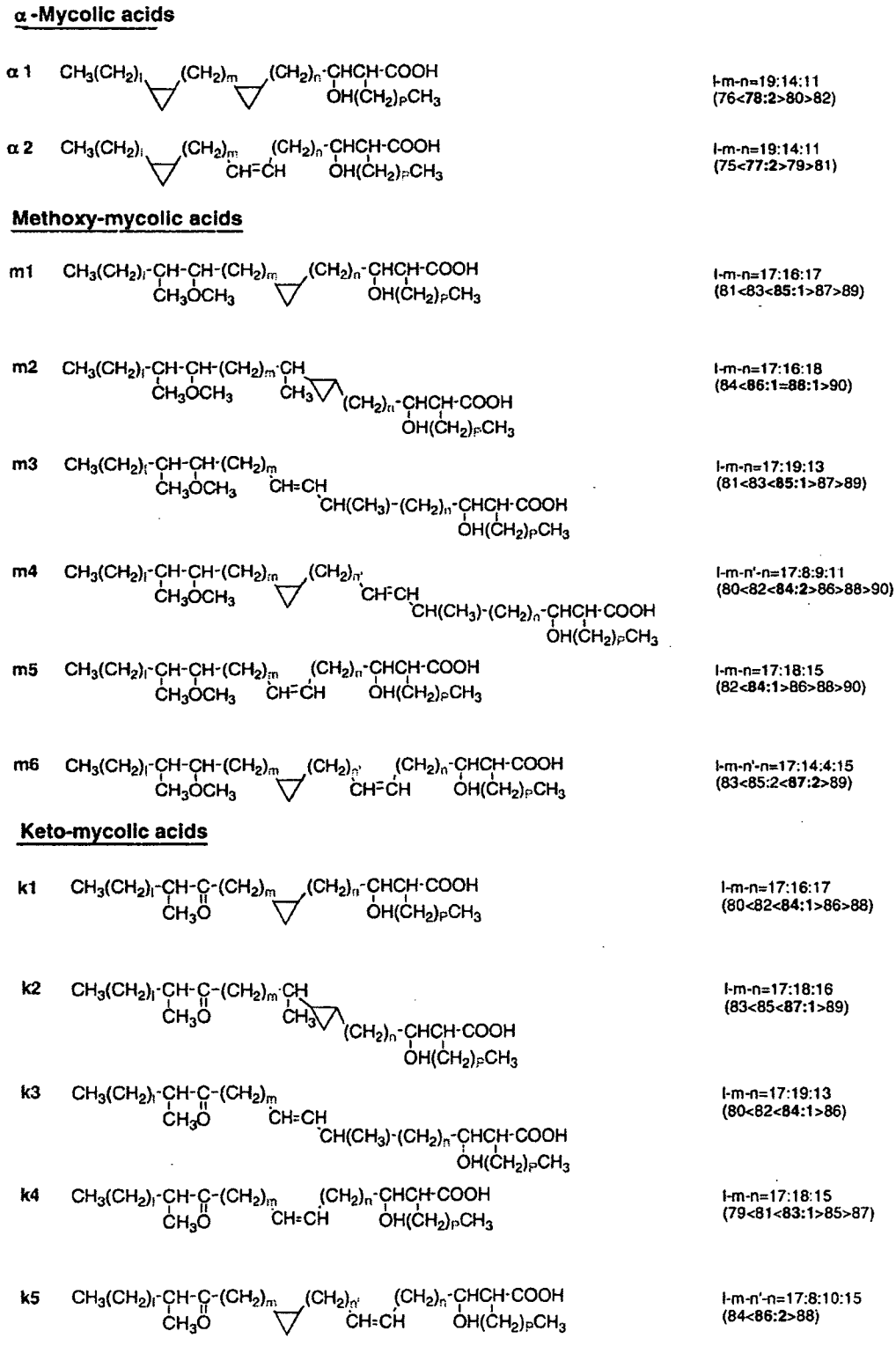


Fig. 1. Structures of 13 subclasses of mycolic acids of CWS from *M. bovis* BCG Tokyo 172 (SMP-105).

SMP-105. In addition, the fact that the ratio of *cis*-to *trans*-form in α-, methoxy-, and keto-mycolates increased in the order 100:0, 91:9, and 71:29 was considered to be another unique characteristic of SMP-105.

Fig. 1 summarizes the possible structures of the thirteen types of mycolic acids separated from SMP-105, based on the chromatographic behaviors, MALDI-TOF and FAB mass analyses, NMR analysis and on deduction based on findings from previous reports (Watanabe et al., 2001, 2002).

## 4. Discussion

Mycolic acids are the most characteristic high molecular weight bioactive lipid component of the mycobacterial cell envelope, and their structures vary greatly according to mycobacterial species, culture conditions, and lipid classes (Minnikin et al., 1984; Kaneda et al., 1986, 1988, 1995; Watanabe et al., 2001, 2002; Fujita et al., 2005a,b; Fujita et al., 2007). As it has been reported that subclass composition of mycolic acids differs among *M. bovis* BCG substrains after multiple passages (Behr et al., 2002), we carefully separated total mycolic acid methyl esters of CWS derived from *M. bovis* BCG Tokyo 172 (SMP-105) by silica gel TLC. As a result, it was clearly demonstrated that three subclasses and thirteen sub-subclasses of mycolic acid methyl esters, including α-, methoxy-and keto-mycolates exist. The separation was satisfactory and this pattern differed from that of *M. bovis* BCG Pasteur or Connaught strains, which possess only α-and keto-mycolic acids. Since the wild strain of *M. bovis* B-10 contains α-, methoxy-and keto-mycolic acids in a ratio of roughly 1:2:1 by weight, the existence of methoxy-mycolates may affect the morphology and immunopotentiating activities of mycoloyl glycolipids, and BCG-CWS may have distinctive immunomodulatory activities (Azuma et al., 1974; Hayashi et al., 1998; Azuma and Seya, 2001). Sub-subclass analysis of α-, methoxy-, and keto-mycolates in SMP-105 was first performed by $AgNO_3$-coated silica gel TLC, which allowed the separation of methyl mycolates into saturated, *cis*-and *trans*-monoenoic, and *cis*-and *trans*-dienoic mycolic acid sub-subclasses. Each spot on $AgNO_3$-coated silica gel TLC was recovered and analyzed by MALDI/TOF and FAB mass spectrometry and NMR. As a result, α-mycolates were separated into *cis*, *cis*-dicyclopropanoic acids centering at $C_{78}$ (α1), and *cis*-monocyclopropanoic-*cis*-monoenoic acids centering at $C_{77}$ (α2). Methoxy-mycolates were grouped into six subclasses: *cis*-monocyclopropanoic acids centering at $C_{85}$ (m1), smaller amounts of *trans*-monocyclopropanoic acids centering at $C_{86}$ and $C_{88}$ (m2), *trans*-monoenoic acids centering at $C_{85}$ (m3), a novel series of *cis*-monocyclopropanoic-*trans*-monoenoic acids centering at $C_{84}$ (diene-equivalent) (m4), *cis*-monoenoic acids centering at $C_{84}$ (m5), and *cis*-monocyclopropanoic-*cis*-monoenoic acids centering at $C_{87}$ (m6). Keto-mycolates were grouped into five subclasses: *cis*-monocyclopropanoic acids centering at $C_{84}$ (k1), a substantial amount of *trans*-monocyclopropanoic acids centering at $C_{87}$ (k2), *trans*-monoenoic acids centering at $C_{84}$ (k3), *cis*-monoenoic acids centering at $C_{83}$ (k4), and *cis*-monocyclopropanoic-*cis*-monoenoic acids centering at $C_{86}$ (diene-equivalent) (k5). Although structure analysis of subclass or molecular species composition of the cellular mycolic acids of *M. bovis* BCG substrains have already been reported (Minnikin et al., 1984; Kaneda et al., 1986, 1988, 1995; Watanabe et al., 2001, 2002), the present report is the first describing the detailed analytical study of the mycolic acid subclass and molecular species composition of SMP-105. Particularly interesting is the existence of six sub-subclasses of methoxy-mycolic acid, and of novel *cis*-monocyclopropanoic-*trans*-monoenoic methoxy-mycolic acid (m4), all of which are entirely lacking in the recently mutated BCG substrains that have appeared after the mma-3 mutation in 1927 (Behr et al., 2000; Belly et al., 2004).Thus, sub-subclass separation and identification of mycolic acids in mycobacterial lipids revealed new information on particular mycolic acid molecules. Recently, we have demonstrated that *M. leprae* cord factor (TDM) contained α-and only one sub-subclass *cis*-monoenoic keto-mycolic acid with 81 or 83 carbon atoms (Kai et al., 2007), although the subclass composition was the same as that of *M. bovis* BCG. On the other hand, as deduced from NMR analysis, the *cis*/*trans*-ratio of the mycolic acid subclass decreased in the order of α->methoxy-> keto-mycolates. Since recent studies have shown that *trans*-cyclopropanation of mycolic acids suppresses *M. tuberculosis*-induced inflammation and virulence (Yuan et al., 1998; Rao et al., 2006), the structure-biological activity relationship should be investigated more precisely. Taken together, presence of keto-mycolic acid, but absence of methoxy-mycolate may affect toxicity, immunogenicity and intracellular persistency in host animals. Although BCG daughter strains have been attenuated over the 80 years that have elapsed since initial passage and their immunological properties have changed, the cell wall skeleton of *M. bovis* BCG Tokyo 172, an early strain of BCG vaccine, still shows potent immunostimulatory activities, and mycolic acids seem to play critical roles. In the near future, comparative studies on the mycolic acid structures and immunopotential activity relationships among mycobacterial species should be established.

## Acknowledgements

We thank Tomoko Sugiyama for her technical assistance and Francis Cinget for NMR analysis.

## Appendix A. Supplementary data

Supplementary data associated with this article can be found, in the online version, at doi:10.1016/j.mimet.2007.11.016.

## References

Akazawa, T., Masuda, H., Saeki, Y., Matsumoto, M., Takeda, K., Tsujimura, K., Kuzushima, K., Takahashi, T., Azuma, I., Akira, S., Toyoshima, K., Seya, T., 2004. Adjuvant-mediated tumor regression and tumor-specific cytotoxic response are impaired in MyD88-deficient mice. Cancer Res. 64, 757–764.

Azuma, I., Seya, T., 2001. Development of immunoadjuvants for immunotherapy of cancer. Int. Immunopharmacol. 1, 1249–1259.

Azuma, I., Ribi, E.E., Meyer, T.J., Zbar, B., 1974. Biologically active components from mycobacterial cell walls. I. Isolation and composition of cell wall skeleton and components $P_3$. J. Natl. Cancer Inst. 52, 95–101.

Beckman, E.M., Porcelli, S.A., Morita, C.T., Behar, S.M., Furlong, S.T., Brenner, M.B., 1994. Recognition of a lipid antigen by CD1-restricted alpha beta+ T cells. Nature 372, 691–694.

Begum, N.A., Ishii, K., Kurita-Taniguchi, M., Tanabe, M., Kobayashi, M., Moriwaki, Y., Matsumoto, M., Fukumori, Y., Azuma, I., Toyoshima, K., Seya, T., 2004. *Mycobacterium bovis* BCG cell-wall specific differentially expressed genes identified by differential display and cDNA subtraction in human macrophages. Infect. Immun. 72, 937–948.

Behr, M.A., Schroeder, B.G., Brinkman, J.N., Slayden, R.A., Barry III, C.E., 2000. A point mutation in the mma3 gene is responsible for impaired methoxymycolic acid production in *Mycobacterium bovis* BCG strains obtained after 1927. J. Bacteriol. 182, 3394–3398.

Belly, A., Alexander, D., Di Pietrantonio, T., Girard, M., Jones, J., Schurr, E., Liu, J., Sherman, D.R., Behr, M.A., 2004. Impact of methoxymycolic acid production by *Mycobacterium bovis* BCG strains. Infect. Immun. 72, 2803–2809.

Bowden, K., Heilbron, I.M., Jones, E.R.H., Weedon, B.C.L., 1946. Researches on acetylenic compounds. Part I. The preparation of acetylenic ketones by oxidation of acetylenic carbinols and glycols. J. Chem. Soc. 39–45.

Brennan, P.J., 2003. Structure, function, and biogenesis of the cell wall of *Mycobacterium tuberculosis*. Tuberculosis 83, 91–97.

Brennan, P.J., Nikaido, H., 1995. The envelope of mycobacteria. Annu. Rev. Biochem. 64, 29–63.

Cheng, C., Gross, M.L., 1998. Fragmentation mechanisms of oxofatty acids via high-energy collisional activation. J. Am. Soc. Mass Spectrom. 9, 620–627.

Hayashi, A., Doi, O., Azuma, I., Toyoshima, K., 1998. Immuno-friendly use of BCG-cell wall skeleton remarkably improves the survival rate of various cancer patients. Proc. Jpn. Acad. 74, 50–55.

Heilbron, I.M., Jones, E.R.H., Sondheimer, F., 1949. Research on acetylenic compounds. Part XV. The oxidation of primary acetylenic carbinols and glycols. J. Chem. Soc. 604–607.

Fujita, Y., Naka, T., Doi, T., Yano, I., 2005a. Direct molecular mass determination of trehalose monomycolate from 11 species of mycobacteria by MALDI-TOF mass spectrometry. Microbiology 151, 1443–1452.

Fujita, Y., Naka, T., McNeil, M.R., Yano, I., 2005b. Intact molecular characterization of cord factor (trehalose 6,6'-dimycolate) from nine species of mycobacteria by MALDI-TOF mass spectrometry. Microbiology 151, 3403–3416.

Fujita, Y., Okamoto, Y., Uenishi, Y., Sunagawa, M., Uchiyama, T., Yano, I., 2007. Molecular and supra-molecular structure related differences in toxicity and granulomatogenic activity of mycobacterial cord factor in mice. Microb. Pathog. 43, 10–21.

Ishii, K., Kurita-Taniguchi, M., Aoki, M., Kimura, T., Kahiwazaki, Y., Matsumoto, M., Seya, T., 2005. Gene-inducing program of human dendritic cells in response to BCG CWS, which reflects adjuvancy required for tumor immunotherapy. Immunol. Lett. 98, 280–290.

Kai, M., Fujita, Y., Maeda, Y., Nakata, N., Izumi, S., Yano, I., Makino, M., 2007. Identification of trehalose dimycolate (cord factor) in *Mycobacterium leprae*. FEBS Lett. 581, 3345–3350.

Laval, F., Laneelle, M.A., Deon, C., Monsarrat, B., Daffe, M., 2001. Accurate molecular mass determination of mycolic acids by MALDI-TOF mass spectrometry. Anal. Chem. 73, 4537–4544.

Matsumoto, M., Seya, T., Kikkawa, S., Tsuji, S., Shida, K., Nomura, M., Kurita-Taniguchi, M., Ohigashi, H., Yokouchi, H., Takami, K., Hayashi, A., Azuma, I., Masaoka, T., Kodama, K., Toyoshima, K., Higashiyama, M., 2001. Interferon gamma-producing ability in blood lymphocytes of patients with lung cancer through activation of the innate immune system by BCG cell wall skeleton. Int. Immunopharmacol. 1, 1559–1569.

McNeil, M.R., 1999. Arabinogalactan in mycobacteria: structure, biosynthesis and genetics. In: Goldberg, Joanna B. (Ed.), Genetics of Bacterial Polysaccharides. CRC Press, Boca Raton, FL, pp. 207–223.

McNeil, M.R., Daffe, M., Brennan, P.J., 1991. Location of the mycolyl ester substituents in the cell walls of mycobacteria. J. Biol. Chem. 266, 13217–13223.

Minnikin, D.E., Parlett, J.H., Magnusson, M., Ridell, M., Lind, A., 1984. Mycolic acid patterns of representatives of *Mycobacterium bovis* BCG. J. Gen. Microbiol. 130, 2733–2736.

Nakajima, H., Kawasaki, K., Oka, Y., Tsuboi, A., Kawakami, M., Ikegami, K., Hoshida, Y., Fujiki, F., Nakano, A., Masuda, T., Wu, F., Taniguchi, Y., Yoshihara, S., Elisseeva, O.A., Oji, Y., Ogawa, H., Azuma, I., Kawase, I., Aozasa, K., Sugiyama, H., 2004. WT1 peptide vaccination combined with BCG-CWS is more efficient for tumor eradication than WT1 peptide vaccination alone. Cancer Immunol. Immunother. 53, 617–624.

Nishikawa, H., Yasaki, S., Yoshimoto, T., Sakatani, M., Itoh, M., Masuno, T., Namba, M., Ogura, T., Hirao, F., Azuma, I., Yamamura, Y., 1978. Effect of BCG cell-wall skeleton immunotherapy on the peripheral blood lymphocytes in patients with lung cancer after radiotherapy. Gann 69, 819–824.

Kaneda, K., Naito, S., Imaizumi, S., Yano, I., Mizuno, S., Tomiyasu, I., Baba, T., Kusunose, E., Kusunose, M., 1986. Determination of molecular species composition of $C_{80}$ or longer-chain α-mycolic acids in *Mycobacterium* spp. by gas chromatography-mass spectrometry and mass chromatography. J. Clin. Microbiol. 24, 1060–1070.

Kaneda, K., Imaizumi, S., Mizuno, S., Baba, T., Tsukamura, M., Yano, I., 1988. Structure and molecular species composition of three homologues series of α-mycolic acids from *Mycobacterium* spp. J. Gen. Microbiol. 134, 2213–2229.

Kaneda, K., Imaizumi, S., Yano, I., 1995. Distribution of $C_{22}$-, $C_{24}$-and $C_{26}$-α-unit-containing mycolic acid homologues in mycobacteria. Microbiol. Immunol. 39, 563–570.

Rao, V., Gao, F., Chen, B., Jacobs Jr., W.R., Glickman, M.S., 2006. *Trans*-cyclopropanation of mycolic acids of trehalose dimycolate suppresses *Mycobacterium tuberculosis*-induced inflammation and virulence. J. Clin. Invest. 116, 1660–1667.

Seya, T., Matsumoto, M., Tsuji, S., Begum, N.A., Nomura, M., Azuma, I., Hayashi, A., Toyoshima, K., 2001. Two receptor theory in innate immune activation: studies on the receptors for bacillus Calmette Guerin-cell wall skeleton. Arch. Immunol. Ther. Exp. 49 (Suppl. 1), S13–S21.

Tomer, K.B., Jensen, N.J., Gross, M.L., 1986. Fast atom bombardment and tandem mass spectrometry for determining structural modification of fatty acids. Anal. Chem. 58, 2429–2433.

Tsuji, S., Matsumoto, M., Takeuchi, O., Akira, S., Azuma, I., Hayashi, A., Toyoshima, K., Seya, T., 2000. Maturation of human dendritic cells by cell wall skeleton of *Mycobacterium bovis* bacillus Calmette-Guerin: involvement of toll-like receptors. Infect. Immun. 68, 6883–6890.

Uenishi, Y., Okada, T., Okabe, S., Sunagawa, M., 2007. Study on the cell wall skeleton derived from *Mycobacterium bovis* BCG Tokyo 172 (SMP-105): establishment of preparation and analytical methods. Chem. Pharm. Bull. 55, 843–852.

Watanabe, M., Aoyagi, Y., Ridell, M., Minnikin, D.E., 2001. Separation and characterization of individual mycolic acids in representative mycobacteria. Microbiology 147, 1825–1837.

Watanabe, M., Aoyagi, Y., Mitome, H., Fujita, T., Naoki, H., Ridell, M., Minnikin, D.E., 2002. Location of functional groups in mycobacterial meromycolate chains; the recognition of new structural principles in mycolic acids. Microbiology 148, 1881–1902.

Yamamura, Y., Azuma, I., Taniyama, T., Sugimura, K., Hirao, F., Tokuzen, R., Okabe, M., Nakahara, W., Yasumoto, K., Ohta, M., 1976a. Immunotherapy of cancer with cell wall skeleton of *Mycobacterium bovis*-Bacillus Calmette-Guerin: experimental and clinical results. Ann. N.Y. Acad. Sci. 277, 209–227.

Yamamura, Y., Ogura, T., Yoshimoto, T., Nishikawa, H., Sakatani, M., 1976b. Successful treatment of the patients with malignant pleural effusion with BCG cell-wall skeleton. Gann 67, 669–677.

Yamamura, Y., Sakatani, M., Ogura, T., Azuma, I., 1979. Adjuvant immunotherapy of lung cancer with BCG cell-wall skeleton (BCG-CWS). Cancer 43, 1314–1319.

Yasumoto, K., Manabe, H., Ueno, M., Ohta, M., Ueda, H., 1976. Immunotherapy of human lung cancer with BCG cell-wall skeleton. Gann 67, 787–795.

Yasumoto, K., Manabe, H., Yanagawa, E., Nagano, N., Ueda, H., Hirota, N., Ohta, M., Nomoto, K., Azuma, I., Yamamura, Y., 1979. Nonspecific adjuvant immunotherapy of lung cancer with cell wall skeleton of *Mycobacterium bovis* Bacillus Calmette-Guerin. Cancer Res. 39, 3262–3267.

Yoo, Y.C., Hata, K., Lee, K.B., Azuma, I., 2002. Inhibitory effect of BCG cell-wall skeletons (BCG-CWS) emulsified in squalane on tumor growth and metastasis in mice. Arch. Pharm. Res. 25, 522–527.

Yuan, Y., Zhu, Y., Crane, D.D., Barry III, C.E., 1998. The effect of oxygenated mycolic acid composition on cell wall function and macrophage growth in *Mycobacterium tuberculosis*. Mol. Microbiol. 29, 1449–1458.